Projected effect of 2000-2050 changes in climate and emissions on aerosol levels in China and associated transboundary transport

Hui Jiang[a,b], Hong Liao[a,*], Havala O. T. Pye[c], , Shiliang Wu[d], Loretta J. Mickley[e], John H. Seinfeld[f], and Xiaoye Zhang[g]

[a]State Key Laboratory of Atmospheric Boundary Layer Physics and Atmospheric Chemistry (LAPC), Institute of Atmospheric Physics, Chinese Academy of Sciences, Beijing, China
[b]Graduate University of Chinese Academy of Sciences, Beijing, China
[c]National Exposure Research Laboratory, Environmental Protection Agency, Research Triangle Park, North Carolina, USA
[d]Department of Geological and Mining Engineering and Sciences and Department of Civil and Environmental Engineering, Michigan Technological University, Houghton, Michigan, USA
[e]School of Engineering and Applied Sciences, Harvard University, Cambridge, Massachusetts, USA
[f]Departments of Chemical Engineering and Environmental Science and Engineering, California Institute of Technology, Pasadena, California, USA
[g]Key Laboratory for Atmospheric Chemistry, Chinese Academy of Meteorological Sciences, CMA, Beijing, China

Corresponding author address:
Prof. Hong Liao
LAPC, Institute of Atmospheric Physics
Chinese Academy of Sciences
Beijing 100029, China
E-mail: hongliao@mail.iap.ac.cn

Abstract

We investigate projected 2000-2050 changes in concentrations of aerosols in China and the associated transboundary aerosol transport by using the chemical transport model GEOS-Chem driven by the Goddard Institute for Space Studies (GISS) general circulation model (GCM) 3 at 4°×5° resolution. Future changes in climate and emissions projected by the IPCC A1B scenario are imposed separately and together through sensitivity simulations. Accounting for sulfate, nitrate, ammonium, black carbon (BC), and organic carbon (OC) aerosols, concentrations of individual aerosol species change by -1.5 to +0.8 $\mu g\ m^{-3}$ and $PM_{2.5}$ levels are projected to change by about 10-20% in eastern China as a result of 2000-2050 change in climate alone. With future changes in anthropogenic emissions alone, concentrations of sulfate, BC, and OC are simulated to decrease because of assumed reductions in emissions, and those of nitrate are predicted to increase because of higher NO_x emissions combined with decreases in sulfate. The net result is a predicted reduction of seasonal mean $PM_{2.5}$ concentrations in eastern China by 1-8 $\mu g\ m^{-3}$ (or 10-40%) over 2000-2050. It is noted that current emission inventories for BC and OC over China are judged to be inadequate at present. Transboundary fluxes of different aerosol species show different sensitivities to future changes in climate and emissions. The annual outflow of $PM_{2.5}$ from eastern China to the western Pacific is estimated to change by -7.0%, -0.7%, and -9.0% over 2000-2050 owing to climate change alone, changes in emissions alone, and changes in both climate and emissions,

respectively. The fluxes of nitrate and ammonium aerosols from Europe and Central Asia into western China increase over 2000-2050 in response to projected changes in emissions, leading to a 10.5% increase in annual inflow of $PM_{2.5}$ to western China with future changes in both emissions and climate. Fluxes of BC and OC from South Asia to China in spring contribute a large fraction of the annual inflow of $PM_{2.5}$. The annual inflow of $PM_{2.5}$ from South Asia and Southeast Asia to China is estimated to change by -8%, +281%, and +227% over 2000-2050 owing to climate change alone, changes in emissions alone, and changes in both climate and emissions, respectively. While the 4°×5° spatial resolution is a limitation of the present study, the direction of predicted changes in aerosol levels and transboundary fluxes still provides valuable insight into future air quality.

1 Introduction

Aerosols are important air pollutants that lead to negative health impacts, reductions in visibility, and changes in climate (Intergovernmental Panel on Climate Change (IPCC), 2007). Concentrations of major atmospheric aerosol species (sulfate, nitrate, ammonium, black carbon, organic carbon, and mineral dust) are especially high in China (Matsui et al., 2009; Tie and Cao, 2010; Qu et al., 2010; Cao et al., 2012), driven by a combination of direct and precursor emissions (Streets et al., 2003) and regional meteorological conditions (Zhang et al., 2010a; Zhu et al., 2012). Estimating future aerosol levels in China is essential in considerations of air quality both over China itself and in the Northern Hemisphere.

In the absence of changes in emissions of primary aerosols as well as aerosol precursors, climate change itself will influence future aerosol levels. For example, coupled climate–chemical transport modeling studies show that climate change alone can lead to increased surface ozone in anthropogenically impacted regions by 1–10 ppbv in summertime over the coming decades, based on the IPCC future scenarios (Jacob and Winner, 2009). This increase is a result of slower transport, enhanced biogenic hydrocarbon emissions, and accelerated decomposition of peroxyacetyl nitrate (PAN) at higher temperatures (Hogrefe et al., 2004; Liao et al., 2006; Murazaki and Hess, 2006; Steiner et al., 2006; Racherla and Adams, 2008; Wu et al., 2008; Jacob and Winner, 2009; Andersson and Engardt, 2010; Chang et al., 2010; Lam et al., 2011; Katragkou et al., 2011; Langner et al., 2012; Reuten et al., 2012; Wang et al., 2013a). A warmer future climate is also predicted to

91 influence aerosol levels over the United States and Europe by as much as 1 μg
92 m^{-3} through altered concentrations of atmospheric oxidants, by changed
93 precipitation and boundary layer height, and by shifting gas-particle equilibria
94 (Liao et al., 2006; Unger et al., 2006; Bauer et al., 2007; Jacob and Winner, 2009;
95 Pye et al., 2009; Day and Pandis, 2011; Lam et al., 2011; Tai et al., 2012a; Tai et
96 al., 2012b; Juda-Rezler et al., 2012). Because of the enormous importance of
97 China as a source of aerosols, a study that addresses how aerosol levels in China
98 may change over the coming decades is called for.

99 Another issue that is associated with the aerosol levels in China is the future
100 transboundary aerosol transport. A number of observational and modeling
101 analyses have demonstrated the importance of present-day long-range transport
102 of aerosols from East Asia. Surface observations at island sites (Huebert et al.,
103 2001; Prospero et al., 2003) and aircraft observations in Asian outflow over the
104 Northwest Pacific (Jordan et al., 2003; Maxwell-Meier et al., 2004) and the
105 Northeast Pacific (Clarke et al., 2001; Price et al., 2003) have documented the
106 spring maximum in transpacific transport. By using the global atmospheric
107 chemical transport model GEOS-Chem, Park et al. (2003) predicted that
108 transpacific transport contributes to about 10% of the annual mean natural
109 background surface-layer concentrations of black carbon over the United States.
110 By using satellite measurements of aerosol optical depth over the North Pacific
111 together with GEOS-Chem simulation, Heald et al. (2006) showed that transport
112 from Asia led to a seasonal mean increase of surface-layer sulfate concentration
113 of 0.16 μg m^{-3} (with 50% uncertainty) in the northwestern United States in spring

of 2001. Chin et al. (2007) predicted an enhancement of similar magnitude in surface-layer sulfate aerosol in the western United States in 2001 by long-range aerosol transport; the annual mean contribution to sulfate concentration was estimated to be 0.1-0.2 $\mu g\ m^{-3}$ using the global model GOCART. Yu et al. (2008) performed a satellite-based assessment of transpacific transport of anthropogenic and biomass burning aerosols based on 2002-2005 aerosol optical depths from the Moderate Resolution Imaging Spectroradiometer (MODIS). They estimated that about 25% of aerosol mass exported from East Asia to the northwestern Pacific Ocean can reach the west coast of North America. Two studies examined aerosol transport from Europe and South Asia to China. Chin et al. (2007) estimated that European emissions can increase the surface ammonium sulfate concentrations over eastern Asia by 0.2-0.5 $\mu g\ m^{-3}$. Using the GEOS-Chem model, Zhang et al. (2010b) estimated that organic carbon aerosol from South Asia contributed 50–70% of OC mass over southern China and 20–50% of OC over the western North Pacific in the middle troposphere in summer of 1998.

We present here a study to estimate: (1) the changes of aerosol levels in China over the years 2000-2050 as a result of projected changes in emissions and climate, (2) the changes of transboundary fluxes of aerosols into or out of China over this time period. This study builds on two previous ones. Liao et al. (2007) used the Goddard Institute for Space Studies (GISS) general circulation model (GCM) 3 to drive GEOS-Chem to simulate climatological present-day aerosol levels in the United States, and Pye et al. (2009) investigated the effects of projected climate and emissions changes on 2000-2050

137 sulfate-nitrate-ammonium aerosols in the United States using the same GISS
138 Model 3/GEOS-Chem combination. As a basis for the present study, the IPCC
139 emission scenario A1B (Nakicenovic and Swart, 2000) is adopted; this scenario
140 represents a future world with rapid economic growth and introduction of new and
141 more energy-efficient technologies. GISS Model 3 global meteorological fields are
142 used to drive the atmospheric chemical transport model GEOS-Chem for both
143 present day (1996–2005) and years 2046–2055. Effects of climate change alone,
144 emission changes alone, and both climate and emissions changes together on
145 aerosol levels and transboundary fluxes are simulated. The models in the present
146 study have a relatively coarse spatial resolution of 4° latitude by 5° longitude,
147 which are not expected to capture the characteristically high concentrations of
148 aerosols in China's major urban areas. Nevertheless, the direction of projected
149 changes in aerosol levels should be correctly predicted.

150 The methods and model setup used to simulate present-day and year 2050
151 aerosols are described in Section 2. Section 3 evaluates simulated present-day
152 concentrations of aerosols in China. Section 4 shows predictions of future aerosol
153 levels over China due to changes in climate alone, emissions alone, and
154 combined climate and emissions changes, and Section 5 estimates future
155 changes in transboundary transport of aerosols to examine inflow to and outflow
156 from China.

2 Methods

2.1 GEOS-Chem/GISS models

The atmospheric chemical transport model, GEOS-Chem (v.7-4-11, http://acmg.seas.harvard.edu/geos/) is driven by the GISS Model 3 meteorological data (Rind et al., 2007). Both the GISS Model 3 and the GEOS-Chem models have a horizontal resolution of 4° latitude by 5° longitude with 23 vertical layers. The interface between GEOS-Chem and the GISS meteorological fields was described by Wu et al. (2007) and Pye et al. (2009), and the same meteorology from the work of Wu et al. (2008) is used here. The GEOS-Chem model includes coupled ozone-NO_x-hydrocarbon (~80 species, ~300 chemical reactions) (Bey et al., 2001) and aerosol chemistry. Aerosol species simulated in the GEOS-Chem model include sulfate ($^{-}$) (Park et al., 2004), nitrate ($^{-}$) (Pye et al., 2009), ammonium ( ), primary organic carbon (OC) and black carbon (BC) (Park et al., 2003), secondary organic aerosol (SOA), sea salt (Alexander et al., 2005), and mineral dust (Fairlie et al., 2007). SOA formation considers the oxidation of isoprene (Henze and Seinfeld, 2006), monoterpenes and other reactive VOCs (ORVOCs) (Liao et al., 2007), and aromatics (Henze et al., 2008). We are focused on future changes in anthropogenic aerosols in this work; the assessment on mineral dust and sea salt aerosols will be our future work.

We perform simulations for four cases: (1) year 2000 climate and emissions, (2) 2050 climate and 2000 anthropogenic emissions of aerosol precursor and aerosols, (3) 2000 climate and 2050 anthropogenic emissions of aerosol

180 precursor and aerosols, and (4) 2050 climate and emissions. Each case is
181 integrated for 10 years (driven by 1996–2005 meteorological fields to represent
182 year 2000 climate or by 2046–2055 meteorology to represent year 2050 climate)
183 following 1 year of model spin-up. All the results presented in this paper are
184 10-year averages. Statistical analysis based on the student's two sample t-test is
185 applied to the meteorological fields and concentrations of the 10-year simulations.

186 **2.2 Emissions**

187 Present-day and year 2050 assumed anthropogenic emissions of aerosol
188 precursor and aerosols are listed in Table 1. Emissions of O_3 precursors
189 (including NO_x, CO, and non-methane volatile organic compounds (NMVOCs))
190 follow those in Wu et al. (2008), and those of NH_3 and SO_2 are taken from Pye et
191 al. (2009). The base year for present-day anthropogenic emissions is 1999 for the
192 United States (Wu et al., 2008) and 1998 elsewhere (Pye et al., 2009). Year 2050
193 anthropogenic emissions of ozone precursors, aerosol precursors, and aerosols
194 from the IPCC A1B scenario were generated by the Integrated Model to Assess
195 the Greenhouse Effect (IMAGE) socioeconomic model using prescribed growth
196 factors for different regions, species, and sources (Streets et al., 2004). Ammonia
197 emissions have an imposed seasonality that was determined as a function of
198 temperature for one base year in this model. In present day, anthropogenic
199 emissions of NO_x, CO, NMVOCs, SO_2, NH_3, OC, and BC in eastern China are
200 estimated to account for 12%, 16%, 12%, 20%, 18%, 10%, and 19%, respectively,
201 of the total global emissions. Relative to the assumed present day, year 2050

anthropogenic emissions of NO_x, CO, NMVOCs, SO_2, NH_3, OC, and BC in eastern China (20°-55°N, 98°-125°E) are estimated to change by +72%, -7%, +86%, -29%, -12%, -40%, and -59%, respectively.

Present-day and year 2050 natural emissions of ozone and aerosol precursors include NO_x from lightning and soil, and biogenic hydrocarbons (Table 2), which are calculated based on the GISS Model 3 meteorological parameters. Lightning NO_x emissions are parameterized based on convective cloud-top height (Price and Rind, 1992; Wang et al., 1998). Soil NO_x emissions are calculated as a function of temperature, wind speed, and precipitation (Yienger and Levy, 1995). Representation of biogenic emissions follows the algorithm of Guenther et al. (1995), which considers light and temperature dependence but does not account for the suppression of isoprene emissions under elevated ambient CO_2 concentrations (Rosenstiel et al., 2003) and climate-induced changes in land-cover. Simulated natural emissions of NO_x and biogenic hydrocarbons in eastern China are estimated to increase, respectively, by +20% and +22% over 2000-2050, with the increases in biogenic emissions resulting mainly from the future increases in temperature.

For both radiative forcing in climate simulation and chemical reactions, present-day methane levels in the model are based on observations and set to 1750 ppb with a 5% inter-hemispheric gradient (Wu et al., 2008). The future (2046-2055) methane level in GEOS-Chem follows the IPCC A1B scenario and is set to 2400 ppb for simulations in which changes in anthropogenic emissions are considered (Pye et al., 2009).

2.3 Projected climate change in China over 2000-2050

Present-day meteorological conditions from the NASA GISS Model 3 were simulated with greenhouse gas levels corresponding to years 1996-2005. Year 2046-2055 climate was obtained from a simulation in which CO_2 and other greenhouse gases follow the IPCC A1B scenario. The GISS Model 3 was coupled with a "Q-flux" ocean as described in Wu et al. (2008). Note that the direct and indirect effects of aerosols were not considered in the simulation of 2000-2050 climate change. We have compared the GISS Model 3 predictions of present-day (1996-2005) temperature, wind, and precipitation with assimilated meteorological parameters for 1996-2005 from the Godard Earth Observing System (GEOS)-4 of the NASA Global Modeling and Assimilation Office (GMAO) (http://acmg.seas.harvard.edu/geos/geos_sim.html). The GISS model captures fairly well the pattern and magnitude of surface air temperatures and zonal winds in China (see Supplementary Material). Both the simulated and assimilated surface air temperatures show higher temperatures in southern China than in northern China and also higher temperatures in eastern China than in western China. The maximum temperatures in southeastern China are simulated to be 280–290 K in DJF, 290–300 K in MAM, 300–310 K in JJA, and 290–300 K in SON, which agree with the assimilated values in all seasons except that the assimilated maximum temperatures in southeastern China are lower than 305 K in JJA. Simulated zonal winds averaged over 100°–120°E longitudes show maximum wind speeds of the jet stream located at 200 hPa altitude of 60, 40, 20, and 30 m s^{-1} in DJF, MAM, JJA, and SON, respectively, which agree closely with the

assimilated values. The present-day precipitation simulated by the GISS model shows larger values in MAM and JJA than in DJF and SON, which agree with the assimilated precipitation, but the model overestimates precipitation in the middle and lower reaches of the Yangtze River in MAM whereas underestimates precipitation in that region in JJA.

Figure 1 shows the projected changes in surface air temperature in China from present day to year 2050 by long-lived greenhouse gases under the IPCC A1B scenario. Over the period 2000-2050, surface air temperatures in December-January-February (DJF) are estimated to have large increases, with values of 1.5-3 K in most places of China and the strongest warming of 3-4 K over the Tibetan Plateau and northeastern China. In other seasons, surface air temperatures are estimated to increase by 1-3 K over a large fraction of China. Warming under scenario A1B is generally predicted to be more pronounced than under scenario B1 and less pronounced than under A2 (IPCC, 2007).

Projected changes in precipitation in China from present day to year 2050 are shown in Fig. 2. Relative to present day, year 2050 precipitation in DJF is estimated to increase by 50-80% in northern China and decrease by about 20% in southern China; note that the present-day precipitation in DJF is the smallest among all seasons. In March-April-May (MAM), year 2050 precipitation is estimated to increase by 20-40% in southern China where the present-day seasonal precipitation is greatest. Precipitation is predicted to generally increase in eastern China in Jun-July-August (JJA) and September-October-November (SON). Note that the projected patterns of precipitation changes (the increases in

271 precipitation in northern China in DJF and the increases in precipitation in eastern
272 China in JJA) from the GISS Model 3 generally agree with those from the IPCC
273 AR4 multi-model predictions for China under the A1B scenario (IPCC, 2007).
274 Projected changes in cloud fraction in China from present day to year 2050 are
275 shown in Fig. 3. Changes in cloud fraction correspond well with the changes in
276 precipitation; decreases (or increases) in clouds are associated with the
277 decreases (or increases) in precipitation (Fig.2).

278 The projected changes in the planetary boundary layer (PBL) depth in China
279 between present day and 2050 are shown in Fig. 4. In a warmer 2050, the PBL
280 depths over the heavily populated eastern China are predicted to generally
281 decrease in MAM and SON (see also Supplementary Material). Reductions in
282 PBL depth are also predicted in northern China in DJF and JJA. Simulated
283 changes in the seasonal mean PBL depth in China are in the range of ±10%. The
284 changes in PBL depth result from the simulated changes in atmospheric
285 temperature (or atmospheric stability); a more unstable atmosphere leads to
286 higher PBL depths.

287

288 **3 Simulated present-day aerosols**

289 **3.1 Model results**

290 Figure 5 shows simulated 1996-2005 seasonal mean concentrations of $^{-}$,
291 $^{-}$, , BC, OC, and $PM_{2.5}$ (sum of $^{-}$, $^{-}$, , BC, and OC) in China.
292 Sulfate exhibits maximum concentrations of 7-9 $\mu g\ m^{-3}$ in JJA and of 5-7 $\mu g\ m^{-3}$ in
293 DJF, MAM, and SON in eastern China. Although strong photochemistry facilitates

maximum sulfate formation in JJA, prevalent precipitation in southern China in JJA (Fig. 2) leads to enhanced wet removal of sulfate in that region. Simulated concentrations of $^{-}$ are generally higher than those of $^{-}$ in eastern China, which is likely caused by the overestimate of NH_3 emissions (Wang et al., 2013b). The highest $^{-}$ concentrations of 9-12 μg m^{-3} are simulated in DJF because of the relatively low temperatures and precipitation. In contrast, high temperatures and large rainfall in JJA lead to the lowest $^{-}$ concentrations. Because of the excess amount of NH_3 in eastern China (Wang et al., 2013b), ammonium aerosol exists predominantly as ammonium sulfate or ammonium nitrate; its concentrations are simulated to be in the range of 3-7 μg m^{-3} in eastern China in all seasons. Predicted BC and OC concentrations are high in DJF and SON and low in MAM and JJA, owing to the seasonal variation of precipitation (Fig. 2). Simulated $PM_{2.5}$ concentrations show the highest values of 18-32 μg m^{-3} in DJF and of 18-28 μg m^{-3} in JJA. In the surface layer, $^{-}$ is predicted to have been the most abundant aerosol species over eastern China in 1996-2005, followed by $^{-}$, , OC, and BC.

3.2 Comparisons of simulated concentrations with measurements

Three previous studies have compared the simulated aerosol concentrations in GEOS-Chem with measurements taken during 2001-2009 in China (Zhang et al., 2010a; Wang et al., 2013b; Fu et al., 2012). At a horizontal resolution of 4° latitude by 5° longitude, Zhang et al. (2010a) found that GEOS-Chem tends to underestimate $PM_{2.5}$ aerosol concentrations in China, because measurements

316 are usually taken in urban areas, whereas the simulated values represent grid cell
317 averages. By using the one-way nested-grid capability of GEOS-Chem with a
318 horizontal resolution of 0.5° latitude by 0.6674° longitude driven by the
319 assimilated meteorological fields, Wang et al. (2013b) found that simulated
320 concentrations of sulfate, nitrate, and ammonium at 22 sites in East Asia exhibited
321 annual biases of -10%, +31%, and +35%, respectively, and Fu et al. (2012)
322 reported that the simulated annual mean concentrations of BC and OC averaged
323 over rural and background sites were underestimated by 56% and 76%,
324 respectively. Underestimation of BC in China was also found in all AEROCOM
325 models (Koch et al., 2009), suggesting that emissions of carbonaceous aerosols
326 are currently underestimated in China.

327 No publicly accessible in situ measurement network of aerosols in China
328 exists (Chan and Yao, 2008). Therefore, we have compiled for model evaluation
329 the monthly or seasonal mean measured concentrations of each aerosol species
330 based on measurements reported in the literature. Most observations were
331 conducted between 2001-2009 at urban sites (such as Beijing, Shanghai, and
332 Guangzhou) and at a few rural sites (such as Fenghuangshan, Gaolanshan, and
333 Lin'an). See Supplementary Material for the locations of measurements. Scatter
334 plots of simulated versus observed seasonal mean sulfate, nitrate, BC, and OC
335 concentrations are displayed in Fig. 6. As anticipated, aerosol concentrations are
336 generally underpredicted; the simulated concentrations of sulfate, nitrate, BC, and
337 OC are about 38%, 68%, 29%, and 19% of the measured values, respectively.
338 One notes the especially low levels of BC and OC simulated, as compared with

339 measurements, indicating the inadequacy of current emission inventories for
340 these species. Comparisons of simulated versus observed concentrations of all
341 aerosol species show relatively high correlation coefficients, with values of R^2
342 ranging from 0.77-0.83. These relatively high R^2 values indicate that the model
343 captures the spatial distributions and seasonal variations of each aerosol species
344 despite the general low bias in simulated concentrations. Again, one should bear
345 in mind that predicted concentrations in this study have been averaged over 4°x5°
346 grid cells.

347 4 Predicted 2000-2050 changes in surface-layer aerosols in China

348 4.1 Effect of changes in climate alone

349 Figure 7 shows the predicted future changes in seasonal mean surface-layer
350 aerosol concentrations as a result of the future changes in climate alone.
351 Simulated changes in concentrations of the aerosol species are within the range
352 of -1.5 to +0.8 μg m^{-3} and exhibit similar spatial patterns in each of the four
353 seasons. Climate-induced changes in concentrations of $^-$, BC, and OC
354 correspond well with the changes in precipitation in all seasons (Fig. 2), with
355 increases (or decreases) in aerosol concentrations over places with decreases (or
356 increases) in precipitation. Predicted reductions in nitrate and ammonium aerosol
357 concentrations also result from the increases in temperature over 2000-2050
358 which lead to the shift of gas-aerosol equilibrium toward the gas phase.

359 As a result of the changes in individual aerosol species, $PM_{2.5}$ concentrations
360 in DJF are predicted to exhibit increases of 1-2.5 μg m^{-3} along east and southeast

coasts of China but decreases of 1.5-2.5 μg m^{-3} in central China. Increases in $PM_{2.5}$ are predicted over a large fraction of eastern China in MAM, with maximum increases in the range of 1-2.5 μg m^{-3}. $PM_{2.5}$ in eastern China shows general decreases of 0.5-1.5 μg m^{-3} in JJA and of 1.5-2.5 μg m^{-3} in SON. These estimated climate-induced changes in $PM_{2.5}$ concentrations over 2000-2050 represent about 10-20% of the present-day values in those regions.

Our simulated climate-induced changes in aerosol concentrations are comparable in magnitude with those reported in other studies for other regions. Based on the IPCC A1B scenario, Tagaris et al. (2007) found a 10% decrease in $PM_{2.5}$ throughout the United States and Pye et al. (2009) reported changes in annually averaged sulfate-nitrate-ammonium of up to 0.61 μg m^{-3} in the United States , as a result of 2000-2050 climate change alone. Under the IPCC A2 scenario, climate change over 2000-2050 alone was found to reduce $PM_{2.5}$ concentrations in the United States by −0.9 μg m^{-3} in the study of Avise et al. (2009). Juda-Rezler et al. (2012) reported that from1991-2000 to 2091-2100 PM_{10} over Central-Eastern Europe generally decrease, by up to 1.5 μg m^{-3} in large scale simulations and up to 3.5 μg m^{-3} in fine scale simulations under the IPCC A1B Scenario.

4.2 Effect of changes in anthropogenic emissions alone

In the IPCC A1B scenario, year 2050 annual anthropogenic emissions of SO_2, BC, and OC in eastern China are predicted to decrease by 29%, 59%, and 40%, respectively, relative to the present-day values. Future concentrations of sulfate,

BC, and OC in China are hence predicted to decrease (Fig. 8). The predicted reductions in sulfate aerosol in eastern China lie within the range of 0.5-3.5 $\mu g\ m^{-3}$ throughout the year. Although the simulated present-day concentrations of BC and OC are lower than those of sulfate, the decreases in BC and OC are 0.5-2 $\mu g\ m^{-3}$ and 0.5-3.5 $\mu g\ m^{-3}$, respectively, in eastern China.

Unlike sulfate, BC, and OC, based on changes in emissions alone, nitrate concentrations are predicted to increase in the future due to changing anthropogenic emissions, with the largest increases of 1-2 $\mu g\ m^{-3}$ in DJF, 3.5-4.5 $\mu g\ m^{-3}$ in JJA, and 2-3.5 $\mu g\ m^{-3}$ in MAM and SON in eastern China. These increases can be explained by the assumed 72% increase in annual anthropogenic NO_x emission over 2000-2050 (Table 1) as well as the fact that the future reductions in SO_2 favor the formation of ammonium nitrate. As a result, ammonium concentrations show increases of about 0.5 $\mu g\ m^{-3}$ over those locations with large increases in nitrate.

The net effect of the changes in all aerosol species owing to changes in emissions alone is an overall decrease in $PM_{2.5}$ concentrations in China except for the Tibet Plateau. Over eastern China, the projected largest decreases in $PM_{2.5}$ as a result of the future changes in emissions are 7.5-8 $\mu g\ m^{-3}$ (or 20-40% relative to the present-day values) in DJF, 1-5 $\mu g\ m^{-3}$ (or 10-30%) in MAM and SON, and 1-3 $\mu g\ m^{-3}$ (or 10-40%) in JJA. As noted, the increase in $PM_{2.5}$ over or near the Tibet Plateau is caused by long-range transport from South Asia.

4.3 Effect of changes in both climate and anthropogenic emissions

Predicted future changes in aerosols as a consequence of future changes in both climate and anthropogenic emissions are summarized in Fig. 9. Concentrations of sulfate, BC, and OC in China are predicted to decrease in all seasons under future changes in both climate and anthropogenic emissions, although climate change can, to some extent, offset the effect of reductions in anthropogenic emissions on these species (Fig. 7). In eastern China, concentrations of sulfate are predicted to decrease 0.5-3.5 $\mu g\ m^{-3}$ in SON and 0.5-2 $\mu g\ m^{-3}$ in other seasons, while those of BC and OC to decrease by 0.5-2 $\mu g\ m^{-3}$ and 0.5-3.5 $\mu g\ m^{-3}$, respectively, in all seasons.

For nitrate aerosol in eastern China, while climate change exerts an effect opposite to that of changes in anthropogenic emissions in DJF, JJA, and SON, the effect of climate change enhances the changes due to emissions in MAM (Fig. 7). As a result of changes in both climate and anthropogenic emissions, concentrations of nitrate in eastern China are predicted to exhibit reductions of 0.5-1 $\mu g\ m^{-3}$ in DJF and increases of 0.5-4.5 $\mu g\ m^{-3}$ in other seasons.

The simulated 2000-2050 changes in $PM_{2.5}$ are dominated by future changes in emissions; concentrations of $PM_{2.5}$ in eastern China are simulated to decrease by 3-7.5 $\mu g\ m^{-3}$ (or 10-30% relative to the present-day values) in DJF, 1-5 $\mu g\ m^{-3}$ (or 30-40%) in JJA, and 3-7.5 $\mu g\ m^{-3}$ (or 20-40%) in SON. In MAM, climate change has a dominant role in influencing the future changes in aerosols in the lower reaches of Yangtze River, where increases of up to 1 $\mu g\ m^{-3}$ in $PM_{2.5}$ are simulated.

With reductions in SO_2, BC, and OC in eastern China over 2000-2050 by 28.5%, 58.6%, and 39.8% (Table 1), respectively, annual mean concentrations of sulfate, BC, and OC over eastern China are simulated to be reduced, respectively, by 19.2%, 56.4%, and 35.9% with future changes in emissions alone whereas by 18.5%, 56.6%, and 36.5% with future changes in both climate and emissions. These results indicate that changes in concentrations of these aerosols are strongly driven by the changes in emissions.

5 Simulated 2000-2050 changes in transboundary transport of aerosols

We next estimate 2000-2050 changes in aerosol fluxes into and out of China. These fluxes of aerosols are calculated through 3 vertical planes from the surface to 100 hPa altitude (Fig. 10): (1) the meridional plane along 135°E from 20° to 55°N that captures the outflow from eastern China to the western Pacific, (2) the meridional plane along 75°E from 35° to 55°N that captures the inflow from Europe and Central Asia to China, and (3) the latitudinal plane along 21.7°N from 90° to 125°E to capture the transport to or from South Asia and Southeast Asia. The transboundary fluxes are calculated within the model at every time step and the seasonal and annual values are presented here.

5.1 Outflow of aerosols from eastern China

5.1.1 Estimated present-day outflow

Simulated present-day seasonal and annual total fluxes of $^{-}$, $^{-}$, , BC, OC, and $PM_{2.5}$ across the meridional plane along 135°E from 20° to 55°N are listed in Table 3. Among all aerosol species, the estimated present-day outflow of

450 $^{-}$ of 5.2 Tg yr^{-1} across this plane is the largest, contributing 48% of the annual
451 outflow of $PM_{2.5}$. The estimated fluxes of $^{-}$, , BC, and OC account for
452 19%, 15%, 5%, and 13% of annual outflow of $PM_{2.5}$, respectively. Aerosol fluxes
453 show strong seasonal variations. The outflow of $^{-}$ is simulated to peak in DJF,
454 which results from the simulated high concentrations of sulfate (Fig. 5) and the
455 strong westerlies (Fig. 11) in that season. All other aerosol species exhibit
456 maximum outflow in MAM, a result that agrees with the conclusions from previous
457 studies (Holzer et al., 2005). Heald et al. (2006) and Chin et al. (2007) reported
458 that the export from Asia is most efficient in spring with nearly all East Asian air
459 involved in transpacific transport. The outflow of aerosols is generally the weakest
460 in JJA, as reported by Holzer et al. (2005) and Yu et al. (2008).

461 The pressure-latitude cross sections of the simulated fluxes of $PM_{2.5}$ at 135°E
462 are shown in Fig. 11. The maximum fluxes of aerosols are found at 500-700 hPa
463 in DJF and SON and at 400-600 hPa in MAM and JJA. The locations of these
464 maximum fluxes shift from 20°-35°N in DJF and MAM to 30°-50°N in JJA and
465 SON, which are consistent with the changes in westerlies (Fig. 11). Our simulated
466 vertical distributions of the strongest fluxes of aerosols agree with those reported
467 by Wang et al. (2009), who showed that the transport to North America occurs
468 mainly in the mid-to-upper troposphere.

469 **5.1.2 Effect of changes in climate alone**

470 Simulated future changes in seasonal and annual fluxes of $^{-}$, $^{-}$, , BC,
471 OC, and $PM_{2.5}$ through the meridional plane along 135°E are also listed in Table 3.

As a result of the climate change alone, the annual fluxes of $^{-}$, $^{-}$, , BC, OC, and $PM_{2.5}$ are simulated to change by -4.2%, -15.6%, -10.1%, 0.0%, -4.5% and -7.0%, respectively, relative to the present-day values. Nitrate aerosol outflow is projected to exhibit the largest reduction, because nitrate aerosol concentrations in China decrease significantly in a warmer climate (Fig. 7). The fluxes of all aerosol species show reductions in all seasons except a small increase (0.7%) in flux of $^{-}$ in MAM.

5.1.3 Effect of changes in anthropogenic emissions alone

Annual fluxes of $^{-}$, $^{-}$, , BC, OC, and $PM_{2.5}$ are simulated to change by -4.6%, +24.6%, +8.3%, -39.6%, -22.4% and -0.7%, respectively (Table 3), as a result of the changes in anthropogenic emissions alone. While nitrate and ammonium outflow fluxes exhibit large increases owing to the projected increases in concentrations in China (Fig. 8), the fluxes of $^{-}$, BC, and OC decrease, corresponding to the future decreases in concentrations of these species (Fig. 8). Consequently, the annual outflow of $PM_{2.5}$ is estimated to exhibit a modest change of -0.7% over 2000-2050 as a result of changes in emissions alone.

5.1.4 Effect of changes in both climate and anthropogenic emissions

Simulated year 2050 outflow fluxes of aerosols through the meridional plane along 135°E from 20° to 55°N with the future changes in both anthropogenic emissions and climate are listed in Table 3. The annual fluxes of $^{-}$, $^{-}$, , BC, OC, and $PM_{2.5}$ are simulated to change by -8.3%, +0.9%, -0.6%, -41.5%, -25.4% and -9.0%, respectively. Climate change mitigates the effects of increases

494 in NO_x emissions on annual fluxes of $^{-}$ and , but slightly enhances the
495 effects of reductions in emissions of SO_2, BC, and OC on outflow of $^{-}$, BC
496 and OC.

497 With all aerosol species accounted for, the 2000-2050 changes in seasonal
498 and annual outflow fluxes of $PM_{2.5}$ resulting from future climate alone always
499 exceed those caused by future changes in emissions alone (Table 3), indicating
500 that future climate change can be influential in estimates of future intercontinental
501 transport of aerosols.

502 It is of interest to examine the rate of nonlinearity of changes in aerosol fluxes
503 with respect to the changes in climate and emissions. The last column of Table 3
504 shows the rate of nonlinearity defined as *NonL*=(Change in flux by climate change
505 alone + Change in flux by changes in emissions alone)/Change in flux by changes
506 in both climate and emissions. Values of *NonL* of seasonal and annual outflow
507 aerosol fluxes mostly deviate from 1.0 (perfect linearity), with absolute values
508 ranging from 0.67 to 9.5.

509 **5.2 Inflow of aerosols to western China**

510 **5.2.1 Present-day inflow**

511 Simulated present-day seasonal and annual fluxes of aerosols through the
512 meridional plane along 75°E from 35° to 55°N are listed in Table 4. On an annual
513 basis, the estimated fluxes of $^{-}$, $^{-}$, , BC, and OC are 2.3, 0.6, 0.6, 0.1,
514 and 0.3 Tg, respectively. The annual inflow of $PM_{2.5}$ is 3.9 Tg, which is about 35%
515 of the annual outflow of $PM_{2.5}$ from eastern China. The inflow of $^{-}$ peaks in

516 DJF, when simulated $^{-}$ concentrations are high in Europe, and in MAM, when
517 the westerlies are strong (Fig. 12). The fluxes of , BC, OC, and $PM_{2.5}$ all peak
518 in MAM because of the dominant effect of strong westerlies in this season. The
519 inflow of $^{-}$ is largest in JJA, when simulated $^{-}$ concentrations are highest
520 in Europe (not shown).

521 The pressure-latitude cross sections of the simulated fluxes of $PM_{2.5}$ at 75°E
522 are shown in Fig. 12. The fluxes of aerosols are the largest north of 40°N, which is
523 the principal predicted transport path from Europe. The strongest inflow of all
524 aerosol species is located at about 700 hPa altitude.

525 **5.2.2 Effect of changes in climate alone**

526 Relative to the present-day values, the annual fluxes of $^{-}$, $^{-}$, , BC,
527 OC, and $PM_{2.5}$ through the meridional plane along 75°E from 35° to 55°N are
528 simulated to change by -0.9%, -25.4%, -11.5%, -7.1%, -6.7%, and -5.9%,
529 respectively, as a result of the climate change alone. As expected, the warmer
530 future temperatures contribute to large reductions of 20-29% in estimated
531 seasonal mean inflow of nitrate. The flux of $^{-}$ is simulated to increase by 5.1%
532 in DJF, as a result of the future stronger westerlies in DJF (Fig. 12). In MAM, JJA,
533 and SON, the westerlies show reductions in wind speed around 700 hPa (Fig.12),
534 leading to reductions in inflow of all aerosol species (Table 4).

535 **5.2.3 Effect of changes in anthropogenic emissions alone**

536 The annual fluxes of $^{-}$, $^{-}$, , BC, OC, and $PM_{2.5}$ are simulated to
537 change by +1.7%, +91.5%, +39.3%, -28.6%, -23.3%, and +19.5%, respectively

(Table 4), as a result of the future changes in anthropogenic emissions alone. The magnitudes of changes in fluxes of $^{-}$, , BC, OC, and $PM_{2.5}$ by anthropogenic emissions alone are generally larger than those of changes by climate change alone on either a seasonal or annual mean basis. As a result of future changes in emissions, the seasonal fluxes of $^{-}$ and show large increases of 68-146% and 25-50%, respectively, those of BC and OC show large decreases of 18-30% and 12-34%, respectively, and the inflow of $PM_{2.5}$ is predicted to increase by about 20% in all seasons (Table 4).

5.2.4 Effect of changes in both climate and anthropogenic emissions

Year 2050 inflow fluxes of aerosols through the meridional plane along 75°E calculated with the future changes in both anthropogenic emissions and climate are listed in Table 4. The annual fluxes of $^{-}$, $^{-}$, , BC, and OC are simulated to change by +0.9%, +49.2%, +27.9%, -29.3%, and -30.0%, respectively. Climate change mitigates the effects of increases in NO_x emissions on annual fluxes of $^{-}$ and , but enhances the effects of changes in emissions of BC and OC. As a net result of the changes in inflow of all aerosol species, the annual inflow of $PM_{2.5}$ to western China is projected to increase by 10.5% over 2000-2050 with future changes in both emissions and climate.

5.3 Transport of aerosols to/from southern China

5.3.1 Present-day transport

The simulated present-day seasonal and annual fluxes of aerosols through the latitudinal plane along 21.7°N from 90°-125°E are listed in Table 5. The annual

560 fluxes of $^{-}$, $^{-}$, , BC, OC, and $PM_{2.5}$ are -0.22, -0.15, -0.09, +0.08,
561 +0.63, and +0.26 Tg, respectively, with the positive (or negative) values indicating
562 northward (or southward) transport of aerosols. The signs of the aerosol fluxes
563 are determined by the directions of winds and the simulated distributions of
564 aerosols. In DJF and SON, while southward fluxes of all aerosol species are
565 found in the lower troposphere over 100°-125°E because of the prevailing
566 northerlies over eastern China, northward fluxes of aerosols are found through the
567 depth of the troposphere over 90°-100°E and in the upper troposphere over
568 100°-125°E (Fig. 13). In MAM and JJA, the southerlies associated with the
569 summer monsoon generally favor northward transport (Fig. 13). The fluxes of
570 aerosols across the southern boundary of China are generally much smaller than
571 those through the eastern and western boundaries. One exception is that the
572 fluxes of BC and OC to China in MAM are amplified as a result of the predominant
573 biomass burning in South Asia in this season (Zhang et al., 2010b).

574 **5.3.2 Effect of changes in climate alone**

575 As a result of the future climate change alone, the changes in annual fluxes of
576 aerosol species are generally small except that the annual southward flux of $^{-}$
577 is simulated to increase by 26.7% relative to the present-day value. The
578 percentage changes in seasonal fluxes are usually much larger. in DJF, the
579 northerlies in the lower troposphere east of 100°E are predicted to be stronger
580 and the southerlies west of 100°E become weaker (Fig. 13), which lead to
581 increases in transport of $^{-}$, $^{-}$, and $PM_{2.5}$ from China to South Asia by 33%,

582 11%, and 67%, respectively. In JJA, the southerlies associated with the summer
583 monsoon are simulated to strengthen in the future climate and hence favor the
584 northward transport of aerosols. The fluxes of all aerosol species to South Asia
585 show reductions in SON, which can be explained by the weaker northerlies in the
586 future atmosphere (Fig. 13).

587 **5.3.3 Effect of changes in anthropogenic emissions alone**

588 The annual fluxes of $^{-}$ and are simulated to change from a net
589 southward outflow to a net northward inflow, as a result of the changes in
590 anthropogenic emissions over 2000-2050 (Table 5). The annual southward flux of
591 $^{-}$ increases by 60%, and the annual northward fluxes of BC, OC, and $PM_{2.5}$
592 increase by 48%, 14%, and 281% , respectively. The annual fluxes of $^{-}$ and
593 exhibit large increases in northward transport because of the large increases
594 in aerosol concentrations in South Asia and Southeast Asia (Fig. 8), and the
595 annual inflow of BC and OC also increases because the reductions in
596 carbonaceous aerosol concentrations in eastern China are projected to be larger
597 than those in South Asia and Southeast Asia (Fig. 8). In contrast, the annual flux
598 of $^{-}$ exhibits southward outflow because of the large increases in $^{-}$ levels
599 in eastern China (Fig. 8).

600 **5.3.4 Effect of changes in both climate and anthropogenic emissions**

601 Simulated fluxes of aerosols through the latitudinal plane along 21.7°N from
602 90°-125°E with the future changes in both anthropogenic emissions and climate

603 are listed in Table 5. The year 2050 annual fluxes of $^{-}$, , BC, OC, and
604 $PM_{2.5}$ are simulated as northward into China, and the annual flux of $^{-}$ is a
605 southward out of China. The 2000-2050 changes in fluxes of all aerosol species
606 are dominated by the contributions from changes in anthropogenic emissions.
607 However, the role of future climate change can exceed that of future changes in
608 emissions for the fluxes of $^{-}$ in DJF, BC in JJA, as well as OC in DJF (Table 5).

609 **6 Conclusions**

610 We estimate changes in aerosol levels in China and the transboundary transport
611 of aerosols in and out of China over the period 2000-2050 by using the global
612 chemical transport model GEOS-Chem with meteorological input from the general
613 circulation model GISS GCM 3 (at 4°×5° resolution) and changes in emissions
614 based on the IPCC A1B scenario.

615 The projected 2000-2050 change in climate alone is estimated to lead to
616 changes in seasonal mean concentrations of individual aerosol species at 4°×5°
617 resolution over China ranging from -1.5 to +0.8 μg m^{-3}. As a result of these
618 changes in individual aerosol species, future $PM_{2.5}$ concentrations in China are
619 simulated to generally decrease, except that increases are predicted along east
620 and southeast coasts of China in DJF and over a large fraction of eastern China in
621 MAM. The simulated climate-induced changes in $PM_{2.5}$ concentrations in China
622 are within ±2.5 μg m^{-3}, which represent about 10-20% of the present-day
623 concentrations in those regions.

As a result of the future changes in anthropogenic emissions alone, concentrations of sulfate, BC, and OC are simulated to decrease by 0.5-3.5 μg m^{-3}, 0.5-2 μg m^{-3}, and 0.5-3.5 μg m^{-3}, respectively, in eastern China. On the contrary, nitrate concentrations are predicted to increase in eastern China over 2000-2050, with the largest increases of 1-2 μg m^{-3} in DJF, 3.5-4.5 μg m^{-3} in JJA, and 2-3.5 μg m^{-3} in MAM and SON. The projected changes in $PM_{2.5}$ owing to the changes in emissions alone show decreases in $PM_{2.5}$ concentrations of 1-8 μg m^{-3} in eastern China over 2000-2050 at a 4°×5° resolution. Under the IPCC A1B scenario, future changes in anthropogenic emissions exert a larger effect on year 2050 $PM_{2.5}$ concentrations in eastern China than does projected future climate change.

The estimated year 2050 transboundary fluxes of aerosol species to and from China are sensitive to future changes in climate and emissions. The present-day flux of $PM_{2.5}$ from eastern China to the western Pacific (through the meridional plane along 135°E from 20° to 55°N) is simulated to be 10.8 Tg yr^{-1}, and the annual outflow of $PM_{2.5}$ is estimated to change by -7.0%, -0.7%, and -9.0%, respectively, over 2000-2050 owing to future climate change alone, future changes in emissions alone, and future changes in both climate emissions. Climate change is predicted to have a larger impact on future fluxes of aerosols than changes in emissions. While annual fluxes of all aerosol species show reductions by climate change alone, future increases in outflow of nitrate and ammonium offset to a large extent the future decreases in outflow of sulfate, BC,

and OC, leading to a small negative change in annual outflow of $PM_{2.5}$ as a result of changes in emissions alone.

The present-day inflow of $PM_{2.5}$ aerosols from Europe and Central Asia to western China (the fluxes through the meridional plane along 75°E from 35° to 55°N) is calculated to be 3.9 Tg yr^{-1}. Over 2000-2050, the fluxes of nitrate and ammonium aerosols are estimated to increase largely as a result of future changes in emissions, leading to an overall 10.5% estimated increase in annual inflow of $PM_{2.5}$ to western China as a result of future changes in both emissions and climate.

The present-day net transport of $PM_{2.5}$ aerosols across the southern boundary (the latitudinal plane along 21.7°N from 90° to 125°E) is estimated as 0.26 Tg yr^{-1}, in which the fluxes of sulfate, nitrate, and ammonium are southward out of China and those of BC and OC are northward into China. Fluxes of BC and OC to China in MAM contribute to a large fraction of the annual inflow of $PM_{2.5}$, as a result of biomass burning in South Asia in this season. The annual net inflow of $PM_{2.5}$ across the southern boundary of China is estimated to change by -8%, +281%, and +227% over 2000-2050 owing to climate change alone, changes in emissions alone, and changes in both climate and emissions, respectively.

Results from the present study indicate that climate change is important to domestic air quality in China as well as long-range transport of aerosols.

Acknowledgements. This work was supported by the Chinese Academy of Sciences Strategic Priority Research Program Grant No. XDA05100503, the National Natural Science Foundation of China under grants 40775083, 40825016, and 41021004, as well as the China Meteorological Administration special funding

671 in atmospheric science GYHY200906020. S. Wu acknowledges support from the
672 U.S. EPA STAR program (grant # 83428601). The U. S. Environmental Protection
673 Agency through its Office of Research and Development collaborated in the
674 research described here. It has been subjected to the Agency's administrative
675 review and approved for publication.
676

References

Alexander, B., Park, R. J., Jacob, D. J., Li, Q. B., Yantosca, R. M., Savarino, J., Lee, C. C.W., and Thiemens, M. H.: Sulfate formation in sea-salt aerosols: constraints from oxygen isotopes, J.Geophys. Res.-Atmos., 110, D10307, doi:10.1029/2004jd005659, 2005.

Andersson, C. and Engardt, M.: European ozone in a future climate: importance of changes in dry deposition and isoprene emissions, J. Geophys. Res.-Atmos., 115, D02303, doi:10.1029/2008jd011690, 2010.

Avise, J., Chen, J., Lamb, B., Wiedinmyer, C., Guenther, A., Salathe, E., Mass, C.: Attribution of projected changes in summertime US ozone and $PM_{2.5}$ concentrations to global changes. Atmos. Chem. Phys., 9, 1111–1124, doi:10.5194/acp-9-1111-2009, 2009.

Bauer, S. E., Koch, D., Unger, N., Metzger, S. M., Shindell, D. T., and Streets, D. G.: Nitrate aerosols today and in 2030: a global simulation including aerosols and tropospheric ozone, Atmos. Chem. Phys., 7, 5043–5059, doi:10.5194/acp-7-5043-2007, 2007.

Bey, I., Jacob, D. J., Yantosca, R. M., Logan, J. A., Field, B. D., Fiore, A. M., Li, Q. B., Liu, H. G. Y., Mickley, L. J., and Schultz, M. G.: Global modeling of tropospheric chemistry with assimilated meteorology: model description and evaluation, J. Geophys. Res.-Atmos., 106, 23073–23095, doi: 10.1029/2001JD000807, 2001.

Cao, J. J., Shen, Z.-X., Chow, J. C., Watson, J. G., Lee, S.-C., Tie, X.-X., Ho, K.-F., Wang, G.-H., and Han, Y.-M.: Winter and summer $PM_{2.5}$ chemical compositions in fourteen Chinese cities, J. Air Waste Manage. Assoc., 62, 1214–1226, doi: 10.1080/10962247.2012.701193, 2012.

Chan, C. K. and Yao, X.: Air pollution in mega cities in China, Atmos. Environ., 42, 1–42, doi:10.1016/j.atmosenv.2007.09.003, 2008.

Chang, H. H., Zhou, J. W., and Fuentes, M.: Impact of climate change on ambient ozone level and mortality in southeastern United States, Int. J. Env. Res. Pub. He., 7, 2866–2880, doi:10.3390/ijerph7072866, 2010.

Chin, Mian, Diehl, T., Ginoux, P., and Malm, W.: Intercontinental transport of pollution and dust aerosols: implications for regional air quality, Atmos. Chem. Phys., 7, 5501–5517, doi:10.5194/acp-7-5501-2007, 2007.

Clarke, A. D., Collins, W. G., Rasch, P. J., Kapustin, V. N., Moore, K., Howell, S., and Fuelberg, H. E.: Dust and pollution transport on global scales: aerosol measurements and model predictions, J. Geophys. Res.-Atmos., 106, 32555–32569, doi:10.1029/2000jd900842, 2001.

Day, M. C. and Pandis, S. N.: Predicted changes in summertime organic aerosol concentrations due to increased temperatures, Atmos. Environ., 45,

6546–6556, doi:10.1016/j.atmosenv.2011.08.028, 2011.
Fairlie, T. D., Jacob, D. J., and Park, R. J.: The impact of transpacific transport of mineral dust in the United States, Atmos. Environ., 41, 1251–1266, doi:10.1016/j.atmosenv.2006.09.048, 2007.
Fu, T. M., Cao, J. J., Zhang, X. Y., Lee, S. C., Zhang, Q., Han, Y. M., Qu, W. J., Han, Z., Zhang, R., Wang, Y. X., Chen, D., and Henze, D. K.: Carbonaceous aerosols in China: top-down constraints on primary sources and estimation of secondary contribution, Atmos. Chem. Phys., 12, 2725–2746, doi:10.5194/acp-12-2725-2012, 2012.
Guenther, A., Hewitt, C. N., Erickson, D., Fall, R., Geron, C., Graedel, T., Harley, P., Klinger, L., Lerdau, M., Mckay, W. A., Pierce, T., Scholes, B., Steinbrecher, R., Tallamraju, R., Taylor, J., and Zimmerman, P.: A global-model of natural volatile organic-compound emissions, J. Geophys. Res.-Atmos., 100, 8873–8892, 1995.
Heald, C. L., Jacob, D. J., Park, R. J., Alexander, B., Fairlie, T. D., Yantosca, R. M., and Chu, D. A.: Transpacific transport of Asian anthropogenic aerosols and its impact on surface air quality in the United States, J. Geophys. Res.-Atmos., 111, D14310, doi:10.1029/2005jd006847, 2006.
Henze, D. K. and Seinfeld, J. H.: Global secondary organic aerosol from isoprene oxidation, Geophys. Res. Lett., 33, L09812, doi:10.1029/2006gl025976, 2006.
Henze, D. K., Seinfeld, J. H., Ng, N. L., Kroll, J. H., Fu, T.-M., Jacob, D. J., and Heald, C. L.: Global modeling of secondary organic aerosol formation from aromatic hydrocarbons: highvs. low-yield pathways, Atmos. Chem. Phys., 8, 2405–2420, doi:10.5194/acp-8-2405-2008, 2008.
Hogrefe, C., Lynn, B., Civerolo, K., Ku, J. Y., Rosenthal, J., Rosenzweig, C., Goldberg, R., Gaffin, S., Knowlton, K., and Kinney, P. L.: Simulating changes in regional air pollution over the eastern United States due to changes in global and regional climate and emissions, J. Geophys. Res.-Atmos., 109, D22301, doi:10.1029/2004jd004690, 2004.
Holzer, M., Hall, T. M., and Stull, R. B.: Seasonality and weather-driven variability of transpacific transport, J. Geophys. Res.-Atmos., 110, D23103, doi:10.1029/2005jd006261, 2005.
Huebert, B. J., Phillips, C. A., Zhuang, L., Kjellstrom, E., Rodhe, H., Feichter, J., and Land, C.: Long-term measurements of free-tropospheric sulfate at Mauna Loa: comparison with global model simulations, J. Geophys. Res.-Atmos., 106, 5479–5492, doi:10.1029/2000jd900627, 2001.
Jacob, D. J. and Winner, D. A.: Effect of climate change on air quality, Atmos. Environ., 43, 51–63, doi:10.1016/j.atmosenv.2008.09.051, 2009.
Jordan, C. E., Dibb, J. E., Anderson, B. E., and Fuelberg, H. E.: Uptake of nitrate and sulfate on dust aerosols during TRACE-P, J. Geophys. Res.-Atmos., 108,

1–10, 8817, doi:10.1029/2002jd003101, 2003.
Juda-Rezler, K., Reizer, M., Huszar, P., Kr¨uger, B. C., Zanis, P., Syrakov, D., Katragkou, E., Trapp, W., Melas, D., Chervenkov, H., Tegoulias, I., and Halenka, T.: Modelling the effects of climate change on air quality over Central and Eastern Europe: concept, evaluation and projections, Clim. Res., 53, 179–203, doi:10.3354/cr01072, 2012.
Katragkou, E., Zanis, P., Kioutsioukis, I., Tegoulias, I., Melas, D., Kr¨uger, B. C., and Coppola, E.: Future climate change impacts on summer surface ozone from regional climate-air quality simulations over Europe, J. Geophys. Res.-Atmos., 116, D22307, doi:10.1029/2011jd015899, 2011.
Koch, D., Schulz, M., Kinne, S., McNaughton, C., Spackman, J. R., Balkanski, Y., Bauer, S., Berntsen, T., Bond, T. C., Boucher, O., Chin, M., Clarke, A., De Luca, N., Dentener, F., Diehl, T., Dubovik, O., Easter, R., Fahey, D.W., Feichter, J., Fillmore, D., Freitag, S., Ghan, S., Ginoux, P., Gong, S., Horowitz, L., Iversen, T., Kirkeva°g, A., Klimont, Z., Kondo, Y., Krol, M., Liu, X., Miller, R., Montanaro, V., Moteki, N., Myhre, G., Penner, J. E., Perlwitz, J., Pitari, G., Reddy, S., Sahu, L., Sakamoto, H., Schuster, G., Schwarz, J. P., Seland, Ø., Stier, P., Takegawa, N., Takemura, T., Textor, C., van Aardenne, J. A., and Zhao, Y.: Evaluation of black carbon estimations in global aerosol models, Atmos. Chem. Phys., 9, 9001–9026, doi:10.5194/acp-9-9001-2009, 2009.
Lam, Y. F., Fu, J. S., Wu, S., and Mickley, L. J.: Impacts of future climate change and effects of biogenic emissions on surface ozone and particulate matter concentrations in the United States, Atmos. Chem. Phys., 11, 4789–4806, doi:10.5194/acp-11-4789-2011, 2011.
Langner, J., Engardt, M., Baklanov, A., Christensen, J. H., Gauss, M., Geels, C., Hedegaard, G. B., Nuterman, R., Simpson, D., Soares, J., Sofiev, M., Wind, P., and Zakey, A.: A multi-model study of impacts of climate change on surface ozone in Europe, Atmos. Chem. Phys., 12, 10423–10440, doi:10.5194/acp-12-10423-2012, 2012.
Liao, H., Chen, W.-T., and Seinfeld, J. H.: Role of climate change in global predictions of future tropospheric ozone and aerosols, J. Geophys. Res., 111, D12304, doi:10.1029/2005jd006852, 2006.
Liao, H., Henze, D. K., Seinfeld, J. H., Wu, S. L., and Mickley, L. J.: Biogenic secondary organic aerosol over the United States: comparison of climatological simulations with observations, J. Geophys. Res.-Atmos., 112, D06201, doi:10.1029/2006jd007813, 2007.
Matsui, H., Koike, M., Kondo, Y., Takegawa, N., Kita, K., Miyazaki, Y., Hu, M., Chang, S. Y., Blake, D. R., Fast, J. D., Zaveri, R. A., Streets, D. G., Zhang, Q., and Zhu, T.: Spatial and temporal variations of aerosols around Beijing in summer 2006: model evaluation and source apportionment, J. Geophys.

796 Res.-Atmos., 114, D00g13, doi:10.1029/2008jd010906, 2009.
797 Maxwell-Meier, K.,Weber, R., Song, C., Orsini, D., Ma, Y., Carmichael, G. R., and
798 Streets, D. G.: Inorganic composition of fine particles in mixed mineral
799 dust-pollution plumes observed from airborne measurements during
800 ACE-Asia, J. Geophys. Res.-Atmos., 109, D19s07,
801 doi:10.1029/2003jd004464, 2004.
802 Murazaki, K., and Hess, P.: How does climate change contribute to surface ozone
803 change over the United States?, J. Geophys. Res.-Atmos., 111, D05301,
804 doi:10.1029/2005jd005873, 2006.
805 Nakicenovic, N. and Swart, R. (Eds.): Special Report on Emissions Scenarios,
806 570 pp., Cambridge Univ. Press, New York, 2000.
807 Park, R. J., Jacob, D. J., Chin, M., and Martin, R. V.: Sources of carbonaceous
808 aerosols over the United States and implications for natural visibility, J.
809 Geophys. Res.-Atmos., 108, 4355, doi:10.1029/2002jd003190, 2003.
810 Park, R. J., Jacob, D. J., Field, B. D., Yantosca, R. M.: Natural and transboundary
811 pollution influences on sulfate-nitrate-ammonium aerosols in the United
812 States: Implications for policy, J. Geophys. Res-Atmos., 109, D15204,
813 doi:10.1029/2003jd004473, 2004.
814 Price, C. and Rind, D.: A simple lightning parameterization for calculating global
815 lightning distributions, J. Geophys. Res.-Atmos., 97, 9919–9933,
816 doi: 10.1029/92JD00719, 1992.
817 Price, H. U., Jaffe, D. A., Doskey, P. V., McKendry, I., and Anderson, T. L.: Vertical
818 profiles of O_3, aerosols, CO and NMHCs in the Northeast Pacific during the
819 TRACE-P and ACE-ASIA experiments, J. Geophys. Res.-Atmos., 108, 8799,
820 doi:10.1029/2002jd002930, 2003.
821 Prospero, J. M., Savoie, D. L., and Arimoto, R.: Long-term record of nss-sulfate
822 and nitrate in aerosols on Midway Island, 1981–2000: evidence of increased
823 (now decreasing?) anthropogenic emissions from Asia, J. Geophys.
824 Res.-Atmos., 108, 4019, doi:10.1029/2001jd001524, 2003.
825 Pye, H. O. T., Liao, H.,Wu, S., Mickley, L. J., Jacob, D. J., Henze, D. K., and
826 Seinfeld, J. H.: Effect of changes in climate and emissions on future
827 sulfate-nitrate-ammonium aerosol levels in the United States, J. Geophys.
828 Res.-Atmos., 114, D01205, doi:10.1029/2008jd010701, 2009.
829 Qu, W. J., Arimoto, R., Zhang, X. Y., Zhao, C. H., Wang, Y. Q., Sheng, L. F., and
830 Fu, G.: Spatial distribution 5 and interannual variation of surface PM10
831 concentrations over eighty-six Chinese cities, Atmos. Chem. Phys., 10,
832 5641–5662, doi:10.5194/acp-10-5641-2010, 2010.
833 Racherla, P. N. and Adams, P. J.: The response of surface ozone to climate
834 change over the Eastern United States, Atmos. Chem. Phys., 8, 871–885,
835 doi:10.5194/acp-8-871-2008, 2008.

Reuten, C., Ainslie, B., Steyn, D. G., Jackson, P. L., and McKendry, I.: Impact of climate change on ozone pollution in the lower Fraser Valley, Canada, Atmos. Ocean., 50, 42–53, doi:10.1080/07055900.2011.643444, 2012.

Rind, D., Lerner, J., Jonas, J., and McLinden, C.: Effects of resolution and model physics on tracer transports in the NASA Goddard Institute for Space Studies general circulation models, J. Geophys. Res.-Atmos., 112, D09315, doi:10.1029/2006jd007476, 2007.

Rosenstiel, T. N., Potosnak, M. J., Griffin, K. L., Fall, R., and Monson, R. K.: Increased CO_2 uncouples growth from isoprene emission in an agriforest ecosystem, Nature, 421, 256–259, doi:10.1038/Nature01312, 2003.

Steiner, A. L., Tonse, S., Cohen, R. C., Goldstein, A. H., and Harley, R. A.: Influence of future climate and emissions on regional air quality in California, J. Geophys. Res.-Atmos., 111, D18303, doi:10.1029/2005jd006935, 2006.

Streets, D. G., Bond, T. C., Carmichael, G. R., Fernandes, S. D., Fu, Q., He, D., Klimont, Z., Nelson, S. M., Tsai, N. Y.,Wang, M. Q.,Woo, J. H., and Yarber, K. F.: An inventory of gaseous and primary aerosol emissions in Asia in the year 2000, J. Geophys. Res.-Atmos., 108, 8809, doi:10.1029/2002jd003093, 2003.

Streets, D. G., Bond, T. C., Lee, T., and Jang, C.: On the future of carbonaceous aerosol emissions, J. Geophys. Res.-Atmos., 109, D24212, doi:10.1029/2004jd004902, 2004.

Tagaris, E., Manomaiphiboon, K., Liao, K.-J., Leung, L.R., Woo, J.-H., He, S., Amar, P., Russell, A.G.: Impacts of global climate change and emissions on regional ozone and fine particulate matter concentrations over the United States. J. Geophys. Res.-Atmos., 112, D14312, doi: 10.1029/2006JD008262, 2007.

Tai, A. P. K., Mickley, L. J., and Jacob, D. J.: Impact of 2000–2050 climate change on fine particulate matter ($PM_{2.5}$) air quality inferred from a multi-model analysis of meteorological modes, Atmos. Chem. Phys., 12, 11329–11337, doi:10.5194/acp-12-11329-2012, 2012a.

Tai, A. P. K., Mickley, L. J., Jacob, D. J., Leibensperger, E. M., Zhang, L., Fisher, J. A., and Pye, H. O. T.: Meteorological modes of variability for fine particulate matter ($PM_{2.5}$) air quality in the United States: implications for PM2.5 sensitivity to climate change, Atmos. Chem. Phys., 12, 3131–3145, doi:10.5194/acp-12-3131-2012, 2012b.

Tie, X. X. and Cao, J. J.: Erratum to “Aerosol pollution in China: Present and future impact on environment”, Particuology, 8, 79–79, doi:10.1016/j.partic.2009.12.001, 2010.

Unger, N., Shindell, D. 5 T., Koch, D. M., Amann, M., Cofala, J., and Streets, D. G.: Influences of man-made emissions and climate changes on tropospheric ozone, methane, and sulfate at 2030 from a broad range of possible futures, J. Geophys. Res.-Atmos., 111, D12313, doi:10.1029/2005jd006518, 2006.

Wang, K., Zhang, Y., Jang, C., Phillips, S., and Wang, B.: Modeling intercontinental air pollution transport over the trans-Pacific region in 2001 using the Community Multiscale Air Quality modeling system, J. Geophys. Res.-Atmos., 114, D04307, doi:10.1029/2008jd010807, 2009.

Wang, Y., Shen, L., Wu, S., Mickley, L. J., He, J., and Hao, J.: Sensitivity of surface ozone over China to 2000–2050 global changes of climate and emissions, Atmos. Environ., 75, 374-382, doi: 10.1016/j.atmosenv.2013.04.045, 2013a.

Wang, Y., Zhang, Q. Q., He, K., Zhang, Q., and Chai, L.: Sulfate-nitrate-ammonium aerosols over China: response to 2000–2015 emission changes of sulfur dioxide, nitrogen oxides, and ammonia, Atmos. Chem. Phys., 13, 2635-2652, doi:10.5194/acp-13-2635-2013, 2013b.

Wang, Y. H., Jacob, D. J., and Logan, J. A.: Global simulation of tropospheric O_3-Noxhydrocarbon chemistry. 1. Model formulation, J. Geophys. Res.-Atmos., 103, 10713–10725, doi: 10.1029/98JD00158, 1998.

Wu, S. L., Mickley, L. J., Jacob, D. J., Logan, J. A., Yantosca, R. M., and Rind, D.: Why are there large differences between models in global budgets of tropospheric ozone?, J. Geophys. Res.-Atmos., 112, D05302, doi:10.1029/2006jd007801, 2007.

Wu, S. L., Mickley, L. J., Leibensperger, E. M., Jacob, D. J., Rind, D., and Streets, D. G.: Effects of 2000–2050 global change on ozone air quality in the United States, J. Geophys. Res.-Atmos., 113, D06302, doi:10.1029/2007jd008917, 2008.

Yienger, J. J. and Levy, H.: Empirical-model of global soil-biogenic NO_x emissions, J. Geophys. Res.-Atmos., 100, 11447–11464, doi: 10.1029/95JD00370, 1995.

Yu, H. B., Remer, L. A., Chin, M., Bian, H. S., Kleidman, R. G., and Diehl, T.: A satellite based assessment of transpacific transport of pollution aerosol, J. Geophys. Res.-Atmos., 113, D14s12, doi:10.1029/2007jd009349, 2008.

Zhang, L., Liao, H., and Li, J. P.: Impacts of Asian summer monsoon on seasonal and interannual variations of aerosols over eastern China, J. Geophys. Res.-Atmos., 115, D00k05, doi:10.1029/2009jd012299, 2010a.

Zhang, L., Liao, H., and Li, J.: Impact of the Southeast Asian summer monsoon strength on the outflow of aerosols from South Asia, Ann. Geophys., 28, 277–287, doi:10.5194/angeo-28-277-2010, 2010b.

Zhu, J. L., Liao, H., and Li, J. P.: Increases in aerosol concentrations over eastern China due to the decadal-scale weakening of the East Asian summer monsoon, Geophys. Res. Lett., 39, L09809, doi:10.1029/2012gl051428, 2012.

Table 1. Present-day and year 2050 (IPCC A1B Scenario) anthropogenic emissions of aerosol precursors and aerosols. The domain of eastern China is (20°-55°N, 98°-125°E).

	Global			Eastern China		
Species	2000	2050	Change,%	2000	2050	Change,%
NO_x (Tg N yr^{-1})						
Aircraft	0.5	0.5	0.0	0.02	0.02	0.0
Anthropogenic	23.7	47.9	+102.0	3.15	6.21	+97.1
Biomass burining	6.5	8.1	+24.6	0.30	0.34	+13.3
Biofuel	2.2	2.1	-4.5	0.53	0.36	-32.1
Fertilizer	0.5	0.9	+80.0	0.06	0.04	-33.3
Total	33.4	59.5	+78.1	4.06	6.97	+71.7
CO (Tg CO yr^{-1})						
Anthropogenic	420.1	413.6	-1.5	104.26	94.04	-9.8
Biomass burining	458.8	749.6	+63.4	21.69	34.46	+58.9
Biofuel	175.6	168.9	-3.8	46.34	31.24	-32.6
Total	1054.5	1332.1	+26.3	172.29	159.74	-7.3
NMVOCs (Tg C yr^{-1})						
Anthropogenic	24.5	42.2	+72.2	2.45	6.52	+166
Biomass burining	3.1	5.1	+64.5	0.14	0.23	+64.3
Biofuel	7.2	6.9	-4.2	1.65	1.12	-32.1
Total	34.8	54.2	+55.7	4.24	7.87	+85.6
SO_2 (Tg S yr^{-1})						
Aircraft	0.1	0.1	0.0	<0.01	<0.01	0.0
Anthropogenic	66.1	88.7	+34.2	13.83	9.81	-29.1
Biomass burining	1.2	2.0	+66.7	0.06	0.09	+50.0
Biofuel	0.3	0.3	0.0	0.07	0.05	-28.6
Ship	4.2	5.4	+28.6	0.03	0.05	+66.7
Total	71.9	96.5	+34.2	13.99	10.00	-28.5
NH_3 (Tg N yr^{-1})						
Anthropogenic	33.3	50.4	+51.4	6.68	5.90	-11.7
Biomass burining	5.9	6.1	+3.4	0.26	0.28	+7.7
Biofuel	1.6	1.7	+6.3	0.32	0.22	-31.3
Total	40.8	58.2	+42.6	7.26	6.40	-11.8
OC (Tg C yr^{-1})						
Anthropogenic	2.5	0.9	-64.0	0.58	0.16	-72.4
Biomass burining	21.6	21.8	+0.9	1.10	1.08	-1.8
Biofuel	6.4	2.7	-57.8	1.31	0.56	-57.3
Total	30.5	25.4	-16.7	2.99	1.80	-39.8
BC (Tg C yr^{-1})						
Anthropogenic	3.1	2.0	-35.5	0.84	0.27	-67.9
Biomass burining	2.6	2.7	+3.8	0.13	0.13	0.0
Biofuel	1.5	0.6	-60.0	0.36	0.15	-58.3
Total	7.2	5.3	-26.4	1.33	0.55	-58.6

925 **Table 2**. Simulated changes in natural emissions due to predicted climate change
926 (IPCC A1B Scenario). The domain of eastern China is (20°–55°N, 98°–125°E).

	Global			Eastern China		
Species	2000	2050	Change,%	2000	2050	Change,%
NO_x (Tg N yr^{-1})						
Lightning	4.8	5.7	+18.8	0.28	0.37	+32.1
Soil	6.7	7.3	+9.0	0.36	0.40	+11.1
Total	11.5	13.0	+13.0	0.64	0.77	+20.3
Biogenic hydrocarbons (Tg C yr^{-1})						
Isoprene	432.4	533.2	+23.3	19.31	23.90	+23.8
Monoterpenes	120.9	144.4	+19.4	6.26	7.38	+17.9
Acetone	43.4	50.4	+16.1	1.28	1.54	+20.3
Propene	12.4	15.2	+22.6	0.55	0.68	+23.6
Methyl Butenol	5.4	6.8	+25.9	1.03	1.30	+26.2
Total	614.5	750.0	+22.1	28.43	34.80	+22.4

927
928
929
930
931
932
933
934
935
936
937
938
939
940
941
942
943
944
945
946
947
948
949
950
951
952

Table 3. Simulated outflow of aerosols from eastern China through the meridional plane along 135°E from 20° to 55°N. Numbers in the parentheses are percentage changes relative to the present-day fluxes. The units are Tg season^{-1} for seasonal fluxes and Tg yr^{-1} for annual fluxes of whole species (e.g., Tg(SO4) season^{-1}, Tg(SO4) yr^{-1}).

		Outflow from Eastern China				
Species		2000[a](Tg)	2050[b](Tg)	2050[c](Tg)	2050[d](Tg)	*NonL*[e]
	DJF	2.12	1.99(-6.1%)	2.07(-2.4%)	1.97(-7.1%)	1.20
	MAM	1.50	1.51(+0.7%)	1.59(+6.0%)	1.58(+5.3%)	1.25
	JJA	0.45	0.43(-4.4%)	0.35(-22.2%)	0.34(-24.4%)	1.09
	SON	1.12	1.04(-7.1%)	0.94(-16.1%)	0.87(-22.3%)	1.04
	Annual	5.19	4.97(-4.2%)	4.95(-4.6%)	4.76(-8.3%)	1.07
	DJF	0.52	0.45(-13.5%)	0.65(+25.0%)	0.50(-3.8%)	-3.00
	MAM	0.86	0.75(-12.8%)	0.89(+3.5%)	0.77(-10.5%)	0.89
	JJA	0.41	0.34(-17.1%)	0.56(+36.6%)	0.46(+12.2%)	1.60
	SON	0.32	0.24(-25.0%)	0.53(+65.6%)	0.40(+25.0%)	1.63
	Annual	2.11	1.78(-15.6%)	2.63(+24.6%)	2.13(+0.9%)	9.50
	DJF	0.45	0.41(-8.9%)	0.48(+6.7%)	0.44(-2.2%)	1.00
	MAM	0.64	0.61(-4.7%)	0.70(+9.4%)	0.67(+4.7%)	1.00
	JJA	0.29	0.25(-13.8%)	0.29(0.0%)	0.26(-10.3%)	1.33
	SON	0.30	0.24(-20.0%)	0.35(+16.7%)	0.30(0.0%)	--
	Annual	1.68	1.51(-10.1%)	1.82(+8.3%)	1.67(-0.6%)	3.00
	DJF	0.17	0.17(0.0%)	0.094(-44.7%)	0.090(-47.1%)	0.95
	MAM	0.21	0.21(0.0%)	0.15(-28.6%)	0.15(-28.6%)	1.00
BC	JJA	0.066	0.066(0.0%)	0.034(-48.5%)	0.033(-50.0%)	0.97
	SON	0.085	0.080(-5.9%)	0.044(-48.2%)	0.041(-51.8%)	1.05
	Annual	0.53	0.53(0.0%)	0.32(-39.6%)	0.31(-41.5%)	0.95
	DJF	0.37	0.34(-8.1%)	0.24(-35.1%)	0.22(-40.5%)	1.07
	MAM	0.64	0.62(-3.1%)	0.58(-9.4%)	0.57(-10.9%)	1.14
OC	JJA	0.17	0.17(0.0%)	0.12(-29.4%)	0.12(-29.4%)	1.00
	SON	0.16	0.15(-6.3%)	0.095(-40.6%)	0.086(-46.3%)	1.01
	Annual	1.34	1.28(-4.5%)	1.04(-22.4%)	1.00(-25.4%)	1.06
	DJF	3.63	3.36(-7.4%)	3.53(-2.8%)	3.22(-11.3%)	0.90
	MAM	3.85	3.70(-3.9%)	3.92(+1.8%)	3.73(-3.1%)	0.67
$PM_{2.5}$	JJA	1.38	1.26(-8.7%)	1.35(-2.2%)	1.22(-11.6%)	0.94
	SON	1.98	1.76(-11.1%)	1.96(-1.0%)	1.69(-14.6%)	0.83
	Annual	10.84	10.08(-7.0%)	10.76(-0.7%)	9.86(-9.0%)	0.86

[a]Seasonal and annual total fluxes averaged over 1996-2005;

[b]Year 2050 fluxes simulated with climate change alone;

[c]Year 2050 fluxes simulated with changes in anthropogenic emissions alone;

961 [d]Year 2050 fluxes simulated with changes in both climate and anthropogenic emissions;

962 [e]$NonL = \frac{- \quad -}{-}$

963

964

965 **Table 4.** Simulated inflow of aerosols to western China through the meridional
966 plane along 75°E from 35° to 55°N. Numbers in the parentheses are percentage
967 changes relative to the present-day fluxes. The units are Tg season^{-1} for seasonal
968 fluxes and Tg yr^{-1} for annual fluxes of whole species (e.g., Tg(SO4) season^{-1},
969 Tg(SO4) yr^{-1}).

		Inflow to Western China				
Species		2000[a](Tg)	2050[b](Tg)	2050[c](Tg)	2050[d](Tg)	*NonL*[e]
	DJF	0.78	0.82(+5.1%)	0.84(+7.7%)	0.84(+7.7%)	1.67
	MAM	0.71	0.67(-5.6%)	0.73(+2.8%)	0.70(-1.4%)	2.00
	JJA	0.27	0.26(-3.7%)	0.23(-14.8%)	0.24(-11.1%)	1.67
	SON	0.53	0.52(-1.1%)	0.53(+0.8%)	0.53(+0.8%)	-0.50
	Annual	2.29	2.27(-0.9%)	2.32(+1.7%)	2.31(+0.9%)	1.00
	DJF	0.075	0.053(-29.3%)	0.15(+100.0%)	0.10(+33.3%)	2.12
	MAM	0.15	0.11(-26.7%)	0.29(+93.3%)	0.22(+46.7%)	1.43
	JJA	0.25	0.19(-24.0%)	0.42(+68.0%)	0.34(+36.0%)	1.22
	SON	0.11	0.088(-20.0%)	0.27(+145.5%)	0.22(+100.0%)	1.25
	Annual	0.59	0.44(-25.4%)	1.13(+91.5%)	0.88(+49.2%)	1.34
	DJF	0.12	0.11(-8.3%)	0.18(+50.0%)	0.17(+41.7%)	1.00
	MAM	0.18	0.16(-11.1%)	0.25(+38.9%)	0.23(+27.8%)	1.00
	JJA	0.16	0.14(-12.5%)	0.20(+25.0%)	0.18(+12.5%)	1.00
	SON	0.15	0.13(-13.3%)	0.22(+46.7%)	0.20(+33.3%)	1.00
	Annual	0.61	0.54(-11.5%)	0.85(+39.3%)	0.79(+27.9%)	1.00
	DJF	0.038	0.038(0.0%)	0.030(-21.1%)	0.030(-21.1%)	1.00
	MAM	0.045	0.043(-4.4%)	0.037(-17.8%)	0.034(-24.4%)	0.91
BC	JJA	0.023	0.022(-4.3%)	0.016(-30.4%)	0.015(-34.8%)	1.00
	SON	0.030	0.029(-3.3%)	0.021(-30.0%)	0.020(-33.3%)	1.00
	Annual	0.14	0.13(-7.1%)	0.10(-28.6%)	0.099(-29.3%)	1.22
	DJF	0.077	0.077(0.0%)	0.054(-29.9%)	0.054(-29.9%)	1.00
	MAM	0.11	0.10(-9.1%)	0.097(-11.8%)	0.090(-18.2%)	1.15
OC	JJA	0.053	0.046(-13.2%)	0.042(-20.8%)	0.036(-32.1%)	1.06
	SON	0.056	0.052(-7.1%)	0.037(-33.9%)	0.033(-41.1%)	1.00
	Annual	0.30	0.28(-6.7%)	0.23(-23.3%)	0.21(-30.0%)	1.00
	DJF	1.08	1.09(+0.9%)	1.25(+15.7%)	1.20(+11.1%)	1.50
	MAM	1.19	1.09(-8.4%)	1.41(+18.5%)	1.28(+7.6%)	1.33
$PM_{2.5}$	JJA	0.75	0.66(-12.0%)	0.91(+21.3%)	0.81(+8.0%)	1.17
	SON	0.87	0.82(-5.7%)	1.08(+24.1%)	1.01(+16.1%)	1.14
	Annual	3.89	3.66(-5.9%)	4.65(+19.5%)	4.30(+10.5%)	1.29

970 [a]Seasonal and annual total fluxes averaged over 1996-2005;

971 [b]Year 2050 fluxes simulated with climate change alone;

972 [c]Year 2050 fluxes simulated with changes in anthropogenic emissions alone;

973 [d]Year 2050 fluxes simulated with changes in both climate and anthropogenic emissions;

974 [e]$NonL = \frac{- \quad -}{-}$

975

976

977 **Table 5.** Simulated transport of aerosols to or from southern China through the
978 latitudinal plane along 21.7°N from 90° to 125°E. Positive (negative) values
979 indicate northward (southward) transport. Percentage change is listed in the
980 parentheses as the 2050 flux has the same sign as 2000 flux. The units are Tg
981 season^{-1} for seasonal fluxes and Tg yr^{-1} for annual fluxes of whole species (e.g.,
982 Tg(SO4) season^{-1}, Tg(SO4) yr^{-1}).

		Transport to or from Southern China				
Species		2000[a](Tg)	2050[b](Tg)	2050[c](Tg)	2050[d](Tg)	*NonL*[e]
	DJF	-0.11	-0.15(+33.4%)	-0.0094(-91.5%)	-0.047(-57.3%)	0.96
	MAM	0.088	0.11(+25.0%)	0.41(+365.9%)	0.43(+388.6%)	1.01
	JJA	-0.011	-0.0051(-53.6%)	0.023(--)	0.047(--)	0.69
	SON	-0.19	-0.16(-15.8%)	-0.13(-31.6%)	-0.11(-42.1%)	1.13
	Annual	-0.22	-0.21(-4.5%)	0.29(--)	0.32(--)	0.96
	DJF	-0.047	-0.052(+10.6%)	-0.050(+6.4%)	-0.059(+25.5%)	0.67
	MAM	0.10	0.045(-55.0%)	0.19(+90.0%)	0.045(-55.0%)	-0.64
	JJA	-0.12	-0.11(-8.3%)	-0.31(+158.3%)	-0.29(+141.7%)	1.06
	SON	-0.086	-0.069(-19.8%)	-0.069(-19.8%)	-0.050(-41.9%)	0.94
	Annual	-0.15	-0.19(+26.7%)	-0.24(+60.0%)	-0.35(+133.3%)	0.65
	DJF	-0.043	-0.054(+25.6%)	-0.0035(-91.9%)	-0.017(-60.5%)	1.10
	MAM	0.066	0.055(-16.7%)	0.22(+233.3%)	0.18(+172.7%)	1.25
	JJA	-0.035	-0.029(-17.1%)	-0.085(+142.9%)	-0.070(+100.0%)	1.26
	SON	-0.073	-0.058(-20.5%)	-0.047(-35.6%)	-0.039(-46.6%)	1.21
	Annual	-0.085	-0.086(+1.2%)	0.085(--)	0.054(--)	1.22
	DJF	-0.00088	-0.0054(+513.6%)	0.013(--)	0.0097(--)	0.88
	MAM	0.095	0.097(+2.1%)	0.11(+15.8%)	0.11(+15.8%)	1.13
BC	JJA	0.0029	0.0043(+48.3%)	0.0039(+34.5%)	0.0050(+72.4%)	1.14
	SON	-0.016	-0.012(-25.0%)	-0.0033(-79.4%)	-0.0017(-89.4%)	1.17
	Annual	0.081	0.084(+3.7%)	0.12(+48.1%)	0.12(+48.1%)	1.08
	DJF	0.076	0.057(-25.0%)	0.090(+18.4%)	0.074(-2.6%)	2.50
	MAM	0.56	0.56(0.0%)	0.63(+12.5%)	0.63(+12.5%)	1.00
OC	JJA	0.017	0.022(+29.4%)	0.0083(-51.2%)	0.011(-35.3%)	0.62
	SON	-0.020	-0.012(-40.0%)	-0.0075(-62.5%)	-0.0046(-77.0%)	1.33
	Annual	0.63	0.63(0.0%)	0.72(+14.3%)	0.71(+12.7%)	1.13
	DJF	-0.12	-0.20(+66.7%)	0.040(--)	-0.040(-66.7%)	1.00
	MAM	0.91	0.87(-4.4%)	1.57(+72.5%)	1.40(+53.8%)	1.27
$PM_{2.5}$	JJA	-0.14	-0.12(-14.3%)	-0.36(+157.1%)	-0.30(+114.3%)	1.25
	SON	-0.39	-0.31(-20.5%)	-0.26(-33.0%)	-0.21(-46.2%)	1.17
	Annual	0.26	0.24(-7.7%)	0.99(+280.8%)	0.85(+226.9%)	1.20

983 [a]Seasonal and annual total fluxes averaged over 1996-2005;

[b]Year 2050 fluxes simulated with climate change alone;

[c]Year 2050 fluxes simulated with changes in anthropogenic emissions alone;

[d]Year 2050 fluxes simulated with changes in both climate and anthropogenic emissions;

[e]$NonL = \frac{- \quad -}{-}$

Figure Captions

Fig. 1. Projected changes in surface air temperature (K) in China from the present day (1996-2005) to future (2046-2055) under the IPCC A1B scenario. Projected changes are all statistically significant at the 95% level, as determined by the student's two sample t-test.

Fig. 2. (a) Simulated precipitation (mm day^{-1}) in China in present day; (b) Projected changes in precipitation (mm day^{-1}) in China from the present day (1996-2005) to future (2046-2055) under the IPCC A1B scenario; (c) The percentage changes in precipitation relative to present day. The dotted areas in (c) are statistically significant at the 95% level, as determined by the student's two sample t-test.

Fig. 3. (a) Simulated cloud fraction (true fraction, 1.0= total overcast cloud) in China in present day; (b) Projected changes in cloud fraction in China from the present day (1996-2005) to future (2046-2055) under the IPCC A1B scenario. The dotted areas in (b) are statistically significant at the 95% level, as determined by the student's two sample t-test.

Fig. 4. (a) Simulated planetary boundary layer (PBL) depth (km) in China in present day; (b) Projected changes in PBL depth (km) in China from the present day (1996-2005) to future (2046-2055) under the IPCC A1B scenario; (c) The percentage changes in PBL depth relative to present day. The dotted areas in (c) are statistically significant at the 95% level, as determined by the student's two sample t-test.

Fig. 5. Simulated present-day seasonal mean surface-layer concentrations (μg m^{-3}) of $^{-}$, $^{-}$, , BC, OC, and $PM_{2.5}$ in China.

Fig. 6. Comparisons of simulated present-day concentrations of sulfate, nitrate, BC, and OC aerosols with measurements. Simulated values are seasonal averages over 1996-2005. Also shown is the 1:1 line (dashed) and linear fit (solid line and equation). R is the correlation coefficient between simulated and measured concentrations.

Fig. 7. Predicted changes in surface-layer concentrations of aerosols (μg m^{-3}) due to changes in climate alone from the present day (1996–2005) to the future (2046–2055). Greenhouse gases follow the IPCC scenario A1B. Anthropogenic emissions are held at present-day values, but natural emissions may change in response to climate. The dotted areas are statistically significant at the 95% level, as determined by the student's two sample t-test.

Fig. 8. Predicted changes in surface-layer concentrations of aerosols (μg m^{-3}) due

to changes in anthropogenic emissions alone from the present day (1996–2005) to the future (2046–2055). Almost all the changes over China are statistically significant at the 95% level, as determined by the student's two sample t-test.

Fig. 9. Predicted changes in surface-layer concentrations of aerosols ($\mu g\ m^{-3}$) due to changes in both climate and anthropogenic emissions from the present day (1996–2005) to the future (2046–2055). Almost all the changes over China are statistically significant at the 95% level, as determined by the student's two sample t-test.

Fig. 10. The locations of the 3 vertical planes through which fluxes of transboundary aerosols are calculated: the meridional plane along 135°E from 20° to 55°N to show the outflow from eastern China to the West Pacific, the meridional plane that along 75°E from 35° to 55°N to show the inflow from Europe and Central Asia to China, and the latitudinal plane along 21.7°N from 90° to 125°E to show the transport to or from South Asia and Southeast Asia.

Fig. 11. (a) Simulated present-day mass fluxes of $PM_{2.5}$ and zonal winds. Projected changes in mass fluxes of $PM_{2.5}$ and zonal winds from the present day (1996-2005) to future (2046-2055) owing to (b) climate change alone, (c) changes in anthropogenic emissions alone, and (d) changes in both climate and anthropogenic emissions. Mass fluxes of $PM_{2.5}$ are shown by shades (Units: Tg) and winds are represented by contours (Units: $m\ s^{-1}$). Both mass fluxes and winds are those through the meridional plane along 135°E from 20° to 55°N. The dotted areas are statistically significant at the 95% level, as determined by the student's two sample t-test.

Fig. 12. Same as Figure 11 but mass fluxes and winds are those through the meridional plane along 75°E from 35° to 55°N.

Fig. 13. (a) Simulated present-day mass fluxes of $PM_{2.5}$ and meridional winds. Projected changes in mass fluxes of $PM_{2.5}$ and meridional winds from the present day (1996-2005) to future (2046-2055) owing to (b) climate change alone, (c) changes in anthropogenic emissions alone, and (d) changes in both climate and anthropogenic emissions. Mass fluxes of $PM_{2.5}$ are shown by shades (Units: Tg) and winds are represented by contours (Units: $m\ s^{-1}$). Both mass fluxes and winds are those through latitudinal plane along 21.7°N from 90° to 125°E. Positive (negative) fluxes indicate northward (southward) transport. The dotted areas are statistically significant at the 95% level, as determined by the student's two sample t-test.

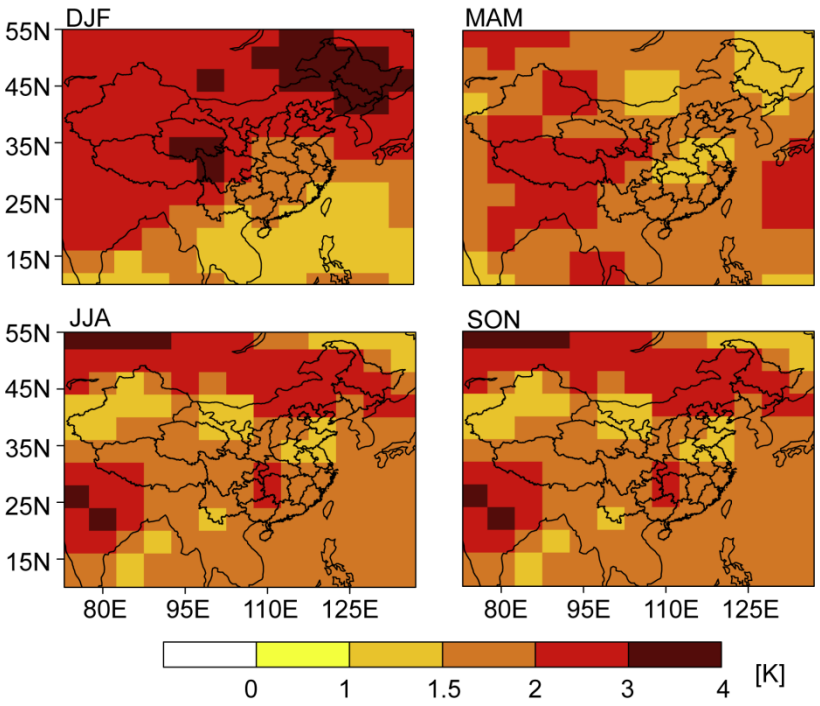

Fig. 1. Projected changes in surface air temperature (K) in China from the present day (1996-2005) to future (2046-2055) under the IPCC A1B scenario. Projected changes are all statistically significant at the 95% level, as determined by the student's two sample t-test.

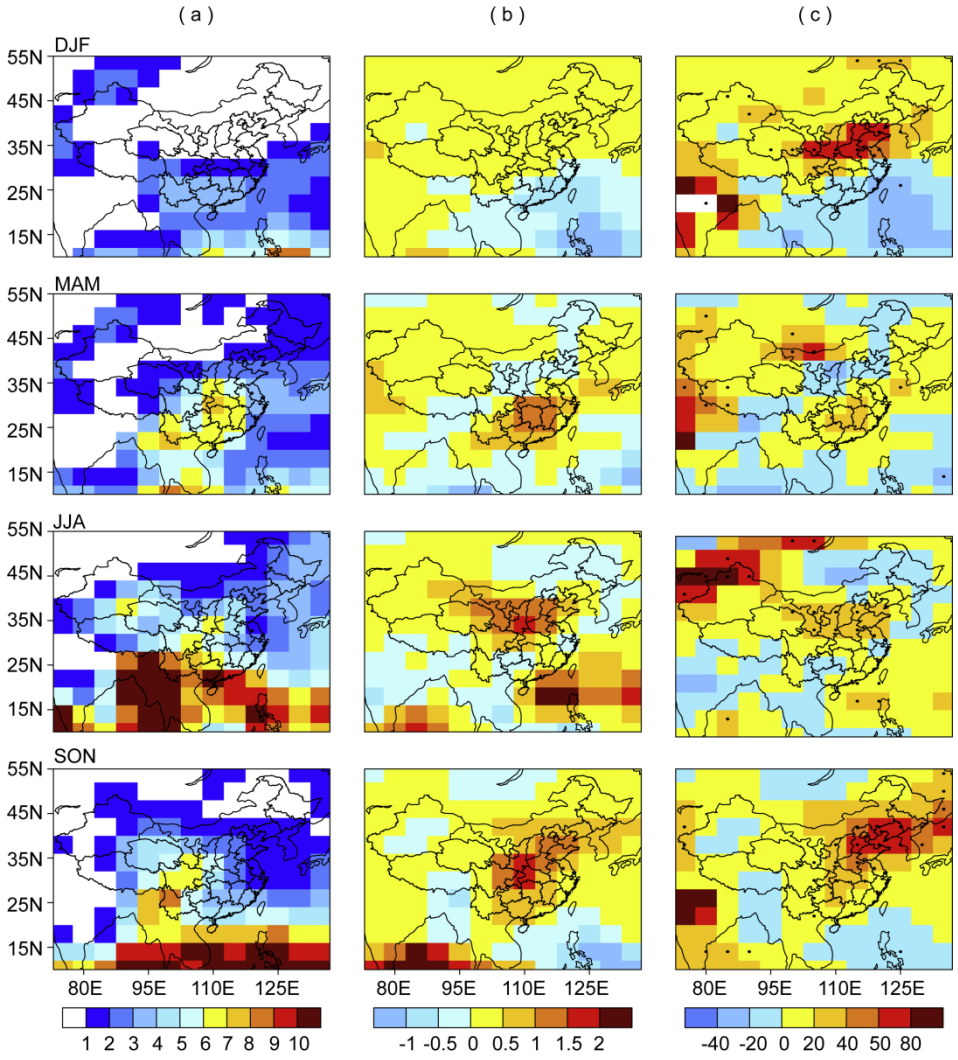

Fig. 2. (a) Simulated precipitation (mm day^{-1}) in China in present day; (b) Projected changes in precipitation (mm day^{-1}) in China from the present day (1996-2005) to future (2046-2055) under the IPCC A1B scenario; (c) The percentage changes in precipitation relative to present day. The dotted areas in (c) are statistically significant at the 95% level, as determined by the student's two sample t-test.

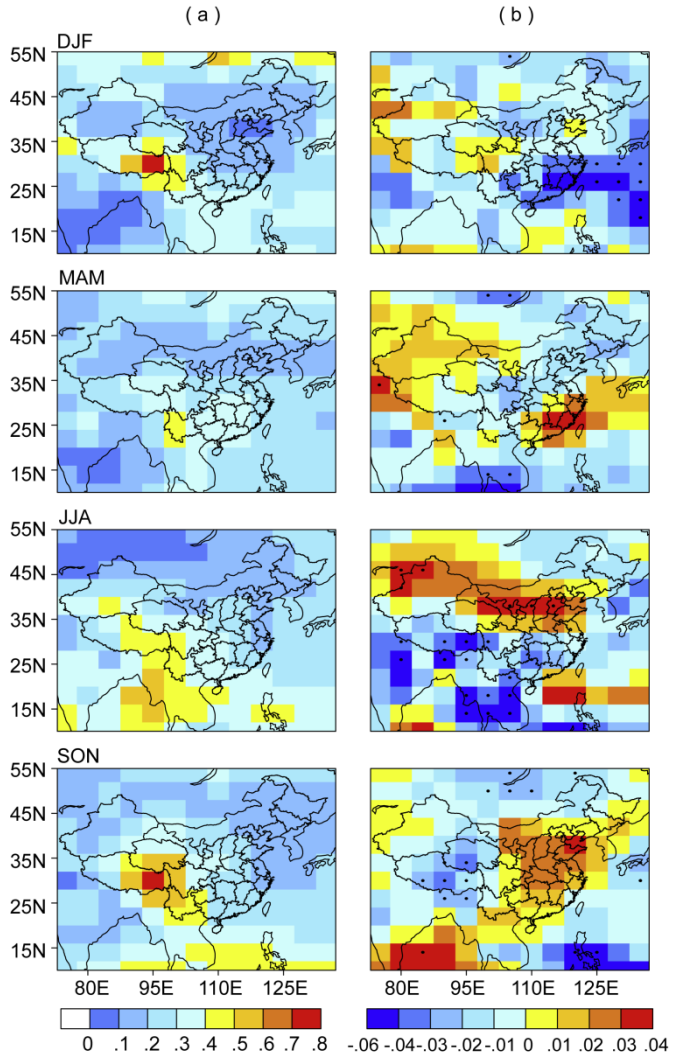

Fig. 3. (a) Simulated cloud fraction (true fraction, 1.0= total overcast cloud) in China in present day; (b) Projected changes in cloud fraction in China from the present day (1996-2005) to future (2046-2055) under the IPCC A1B scenario. The dotted areas in (b) are statistically significant at the 95% level, as determined by the student's two sample t-test.

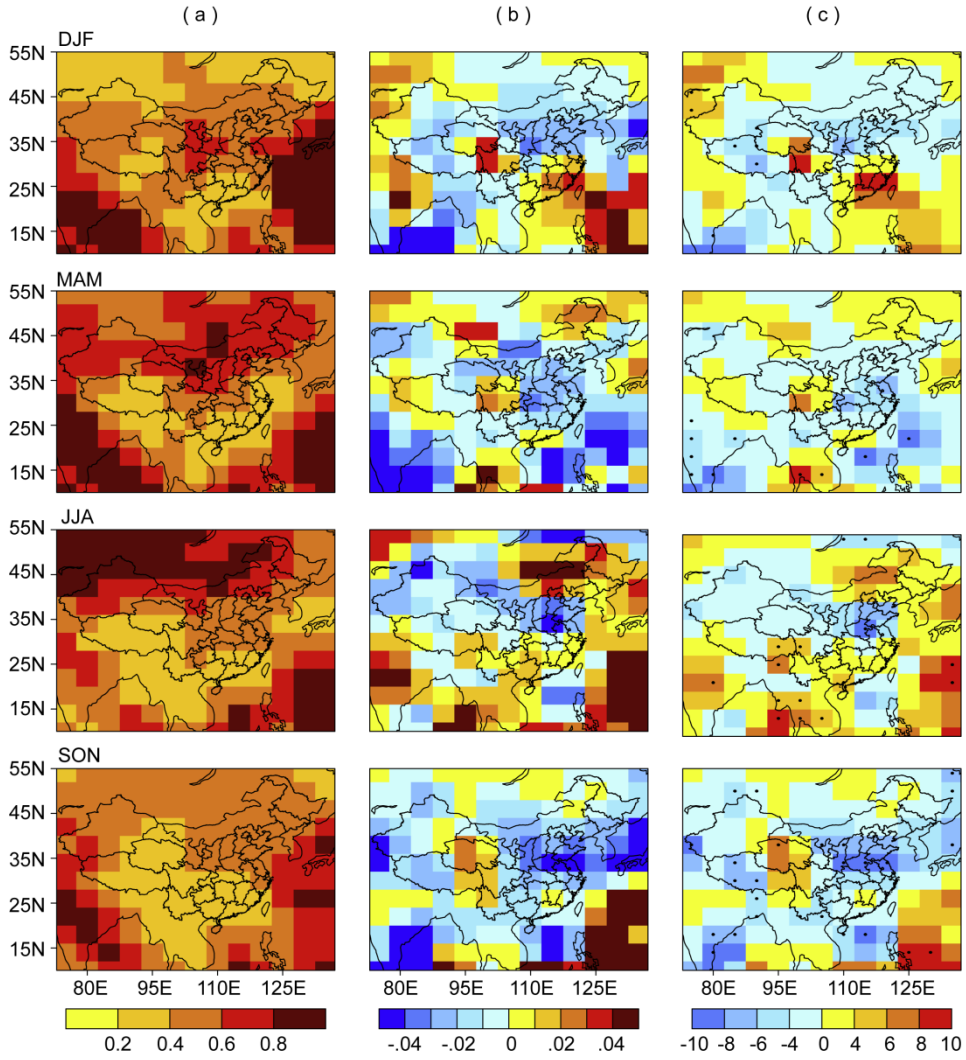

Fig. 4. (a) Simulated planetary boundary layer (PBL) depth (km) in China in present day; (b) Projected changes in PBL depth (km) in China from the present day (1996-2005) to future (2046-2055) under the IPCC A1B scenario; (c) The percentage changes in PBL depth relative to present day. The dotted areas in (c) are statistically significant at the 95% level, as determined by the student's two sample t-test.

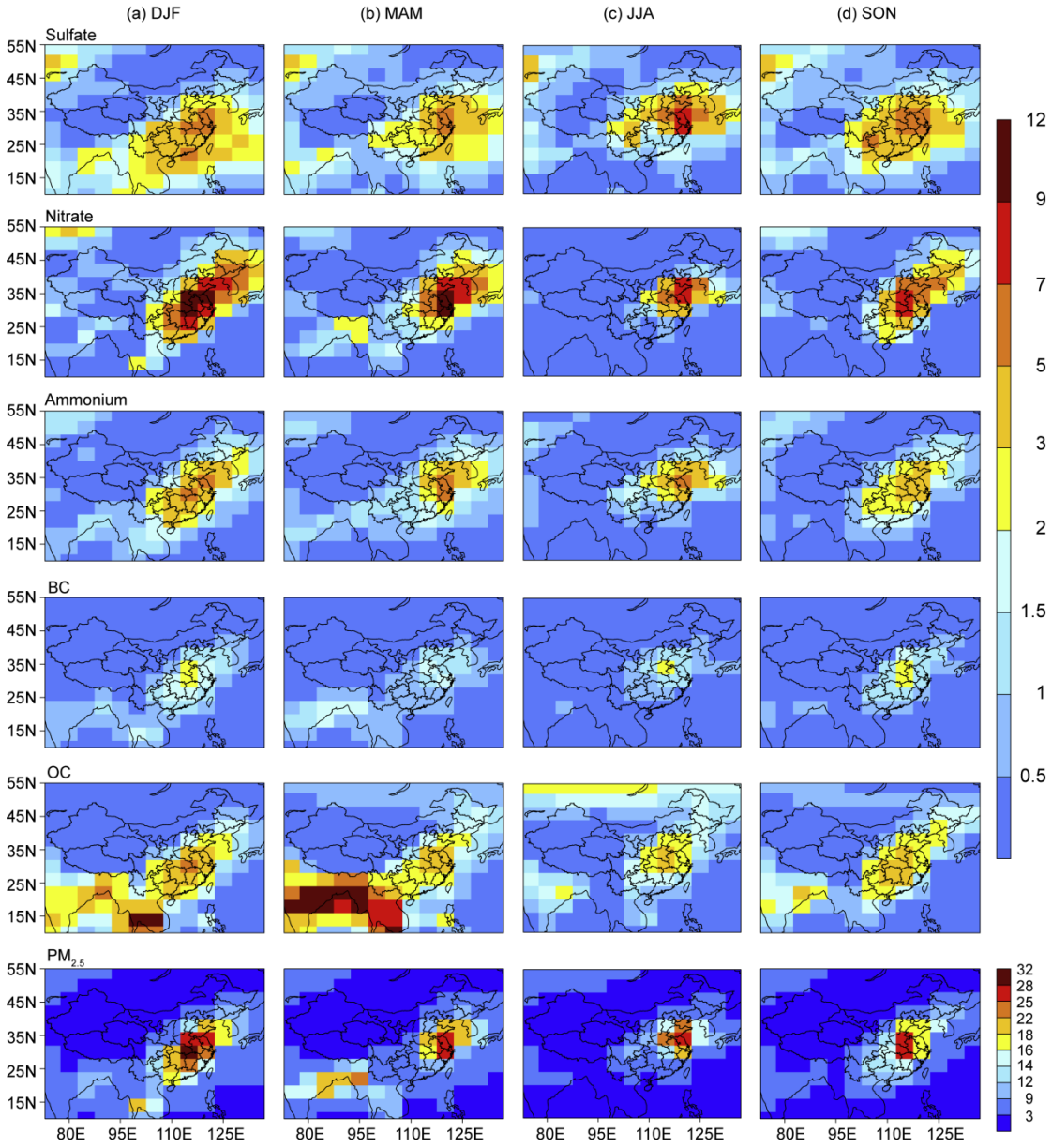

Fig. 5. Simulated present-day seasonal mean surface-layer concentrations (μg m^{-3}) of $^{-}$, $^{-}$, , BC, OC, and $PM_{2.5}$ in China.

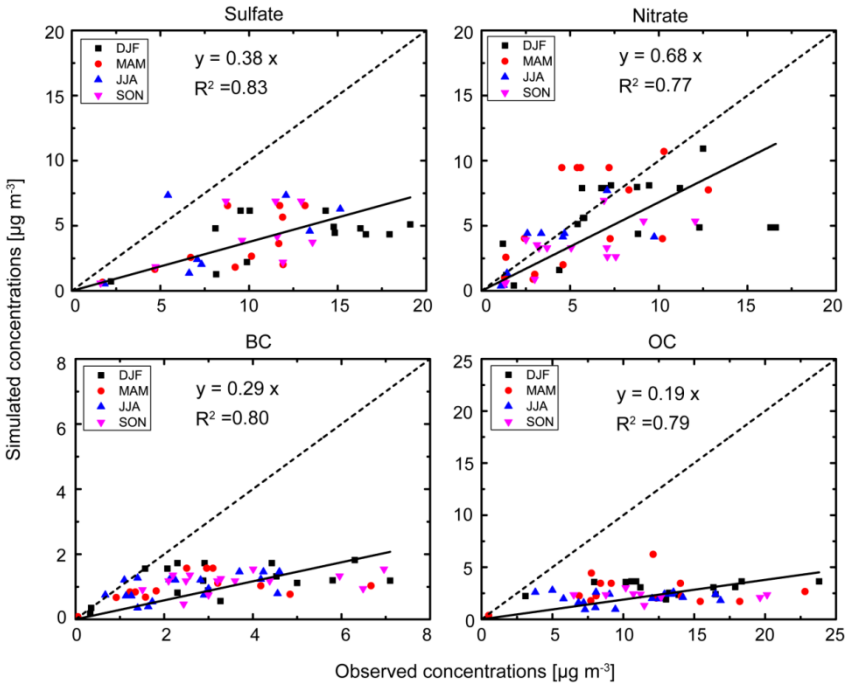

Fig. 6. Comparisons of simulated present-day concentrations of sulfate, nitrate, BC, and OC aerosols with measurements. Simulated values are seasonal averages over 1996-2005. Also shown is the 1:1 line (dashed) and linear fit (solid line and equation). R is the correlation coefficient between simulated and measured concentrations.

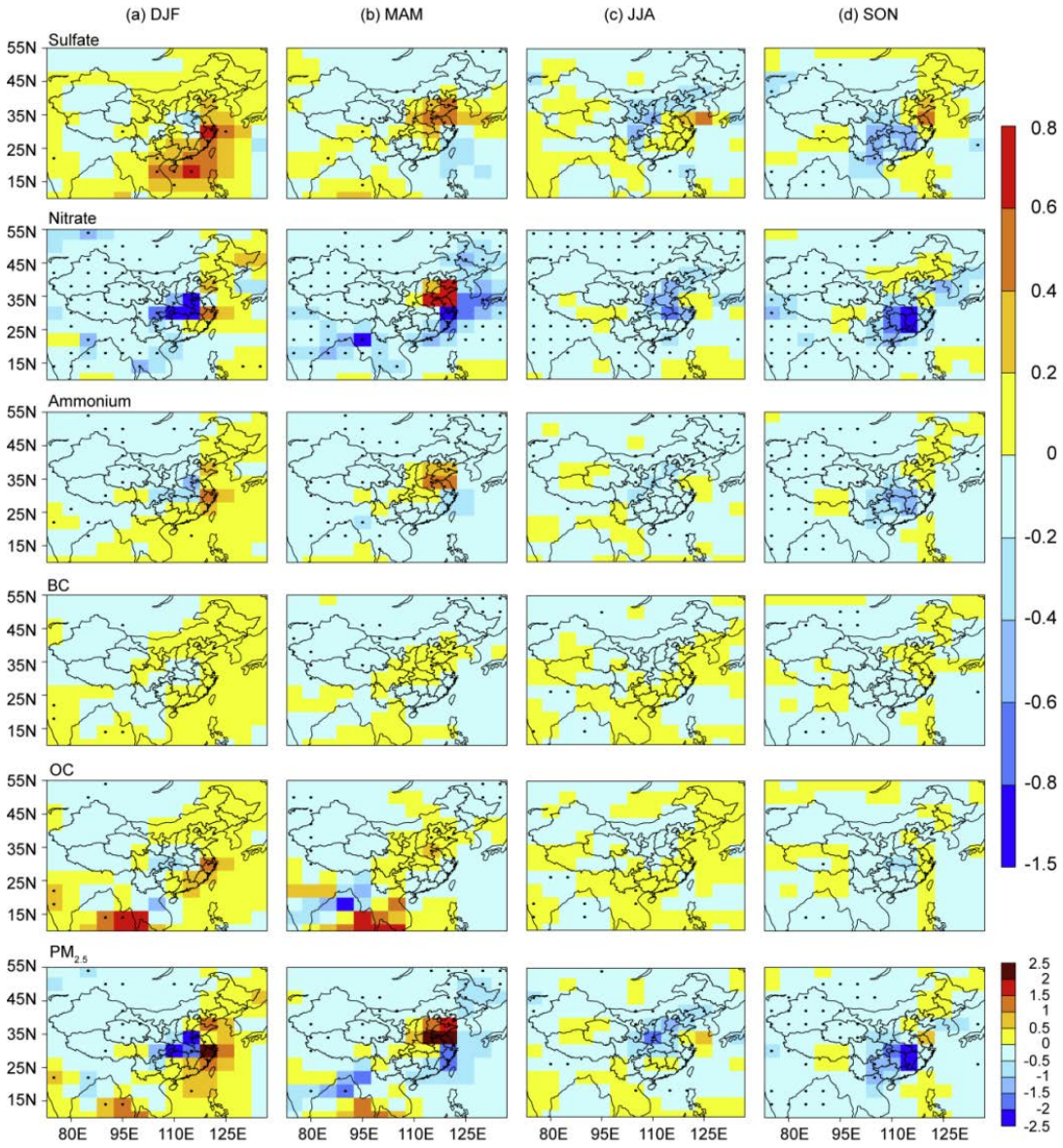

Fig. 7. Predicted changes in surface-layer concentrations of aerosols (μg m^{-3}) due to changes in climate alone from the present day (1996–2005) to the future (2046–2055). Greenhouse gases follow the IPCC scenario A1B. Anthropogenic emissions are held at present-day values, but natural emissions may change in response to climate. The dotted areas are statistically significant at the 95% level, as determined by the student's two sample t-test.

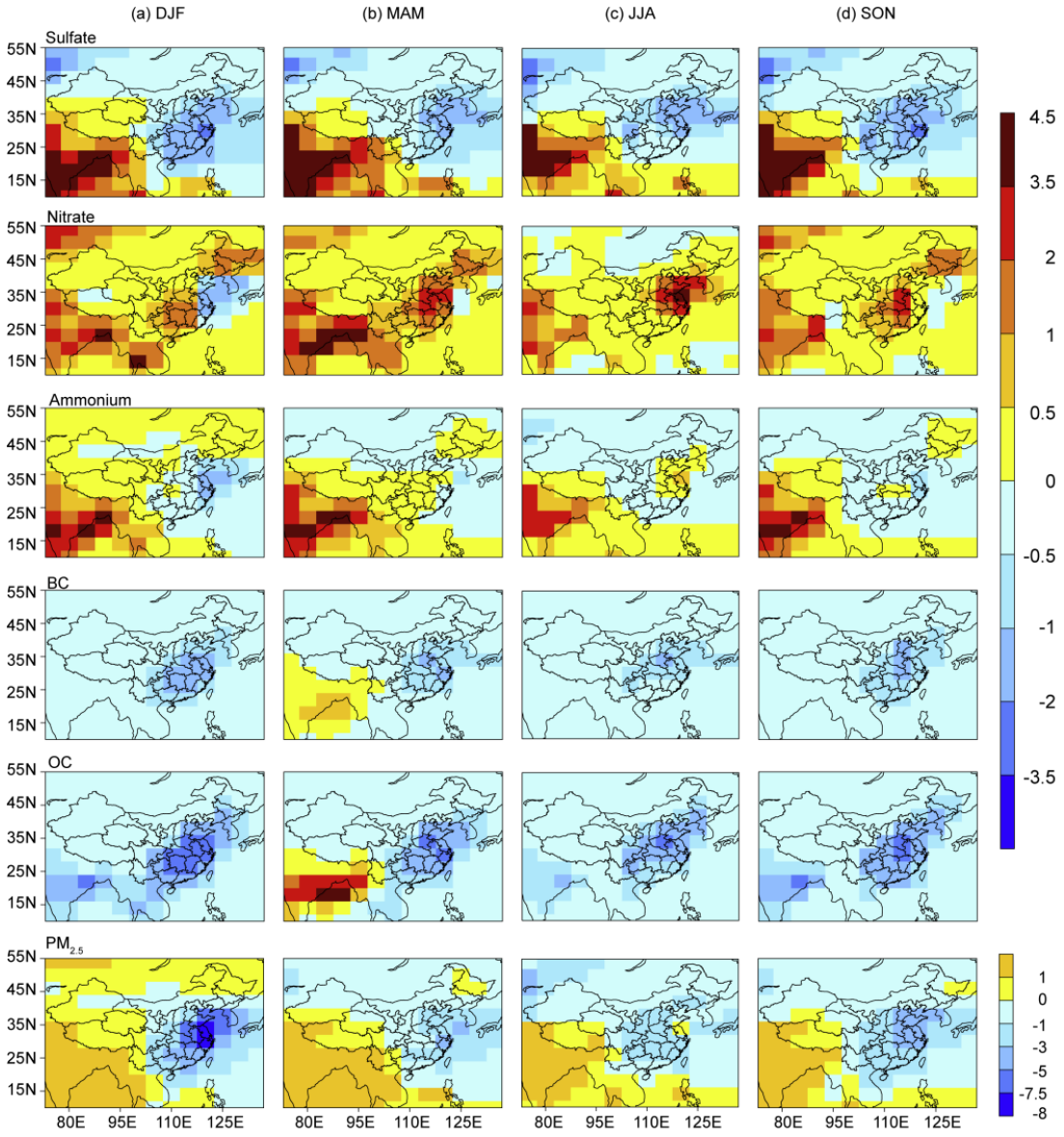

Fig. 8. Predicted changes in surface-layer concentrations of aerosols (μg m^{-3}) due to changes in anthropogenic emissions alone from the present day (1996–2005) to the future (2046–2055). Almost all the changes over China are statistically significant at the 95% level, as determined by the student's two sample t-test.

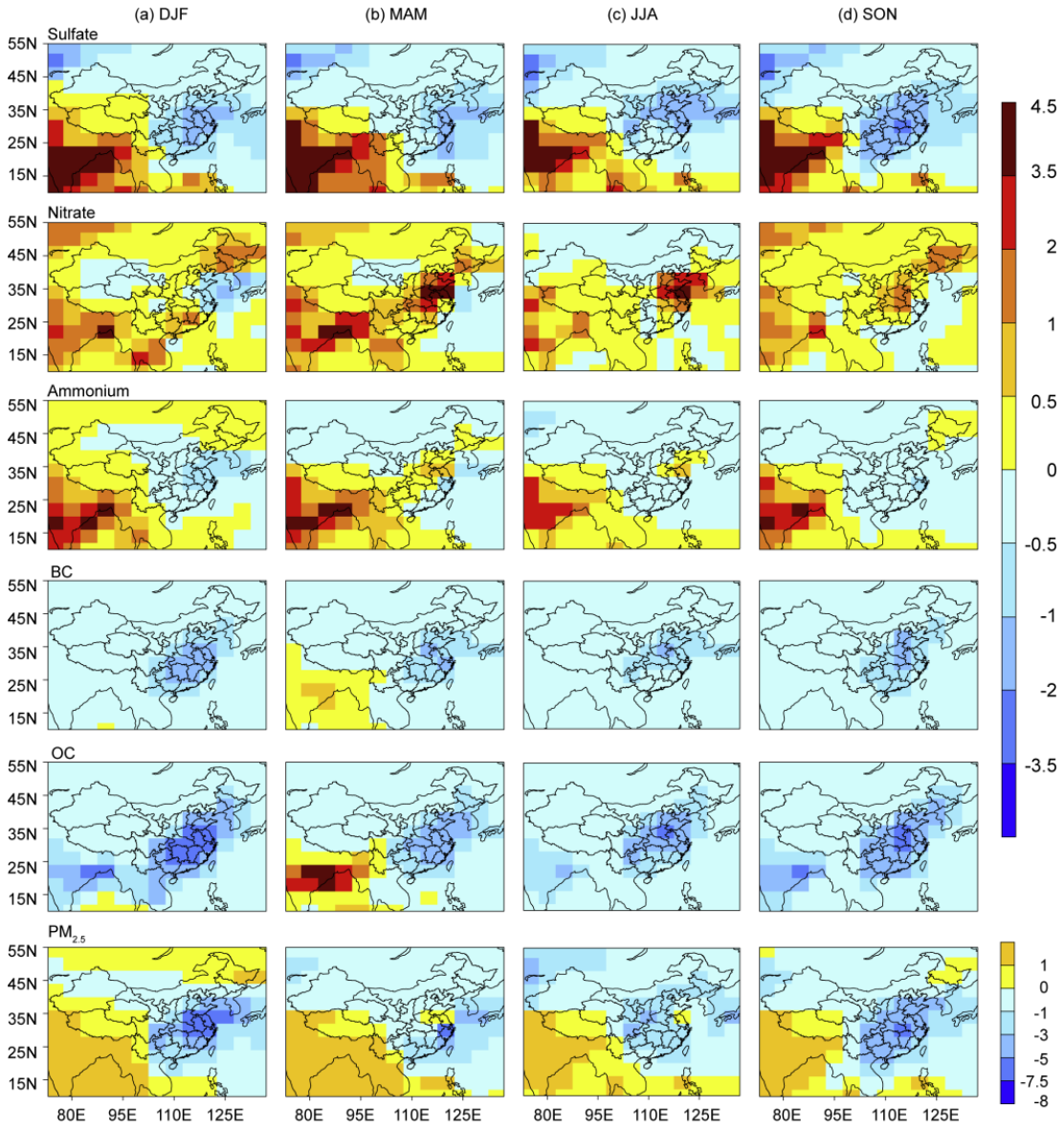

Fig. 9. Predicted changes in surface-layer concentrations of aerosols (μg m^{-3}) due to changes in both climate and anthropogenic emissions from the present day (1996–2005) to the future (2046–2055). Almost all the changes over China are statistically significant at the 95% level, as determined by the student's two sample t-test.

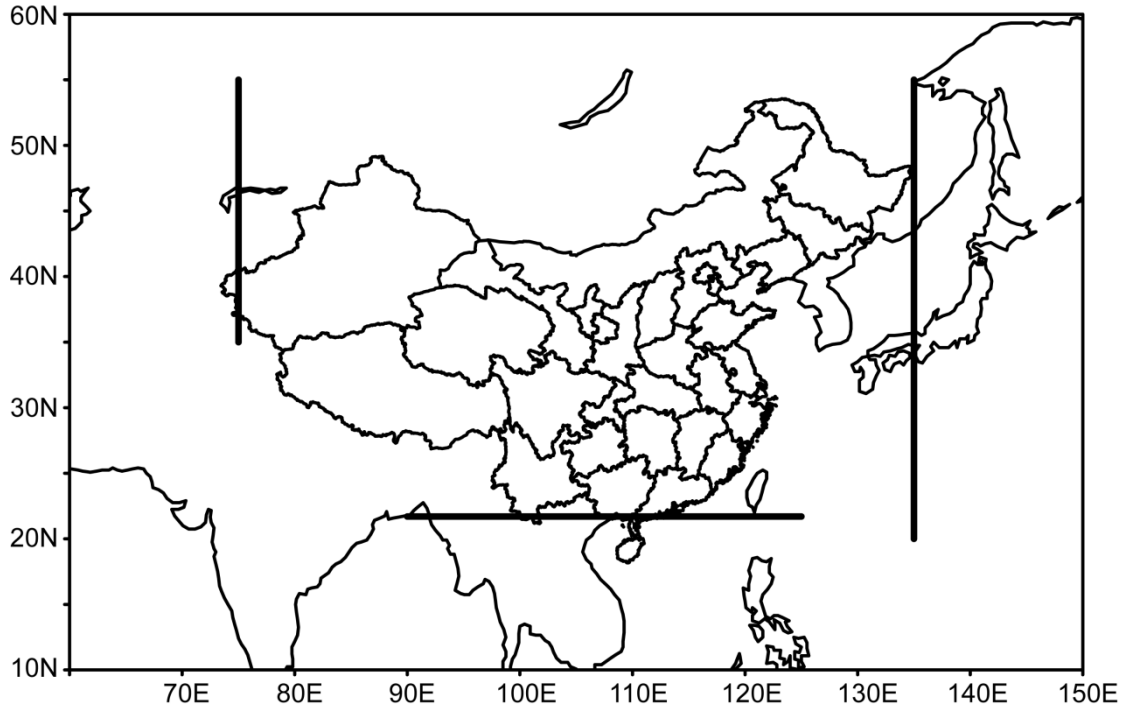

Fig. 10. The locations of the 3 vertical planes through which fluxes of transboundary aerosols are calculated: the meridional plane along 135°E from 20° to 55°N to show the outflow from eastern China to the West Pacific, the meridional plane that along 75°E from 35° to 55°N to show the inflow from Europe and Central Asia to China, and the latitudinal plane along 21.7°N from 90° to 125°E to show the transport to or from South Asia and Southeast Asia.

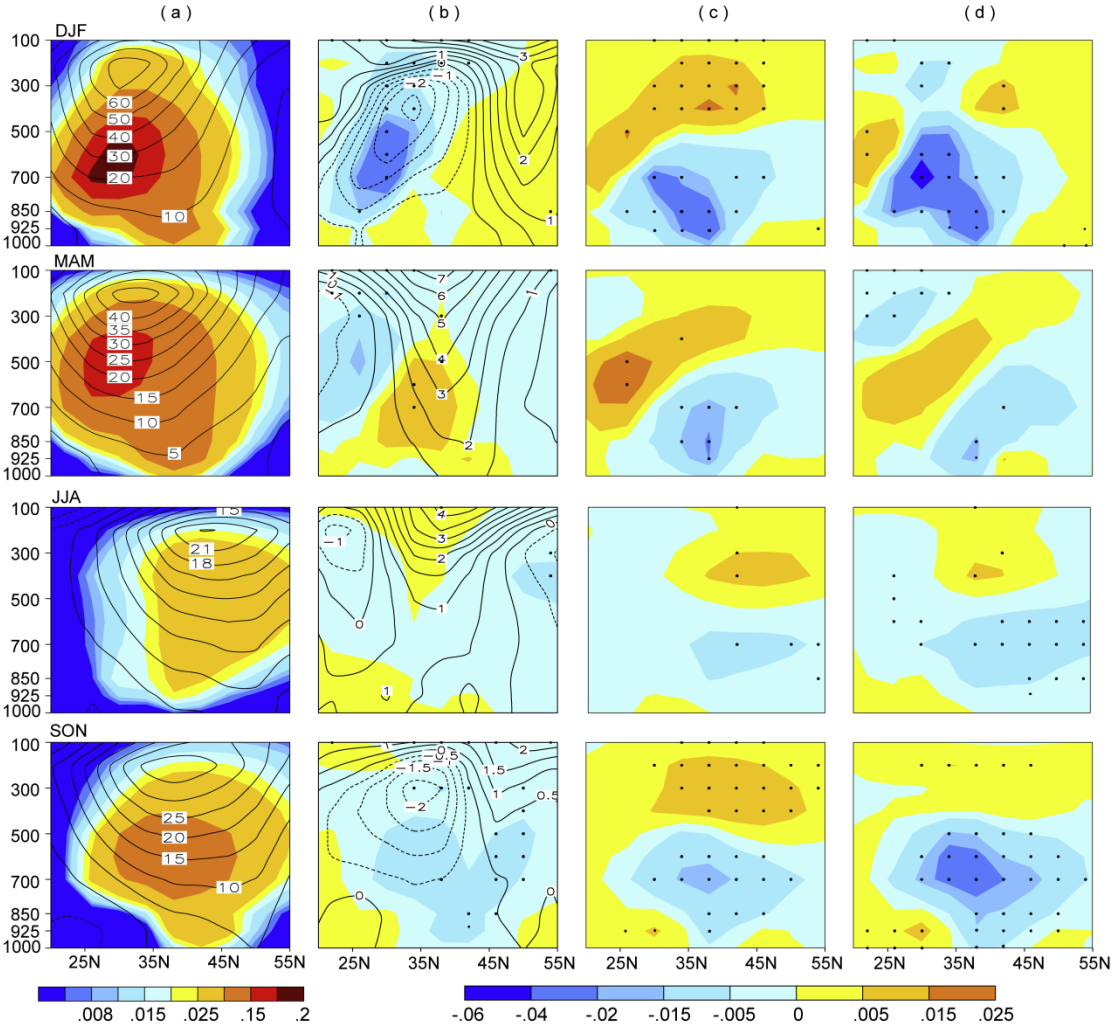

Fig. 11. (a) Simulated present-day mass fluxes of $PM_{2.5}$ and zonal winds. Projected changes in mass fluxes of $PM_{2.5}$ and zonal winds from the present day (1996-2005) to future (2046-2055) owing to (b) climate change alone, (c) changes in anthropogenic emissions alone, and (d) changes in both climate and anthropogenic emissions. Mass fluxes of $PM_{2.5}$ are shown by shades (Units: Tg) and winds are represented by contours (Units: m s^{-1}). Both mass fluxes and winds are those through the meridional plane along 135°E from 20° to 55°N. The dotted areas are statistically significant at the 95% level, as determined by the student's two sample t-test.

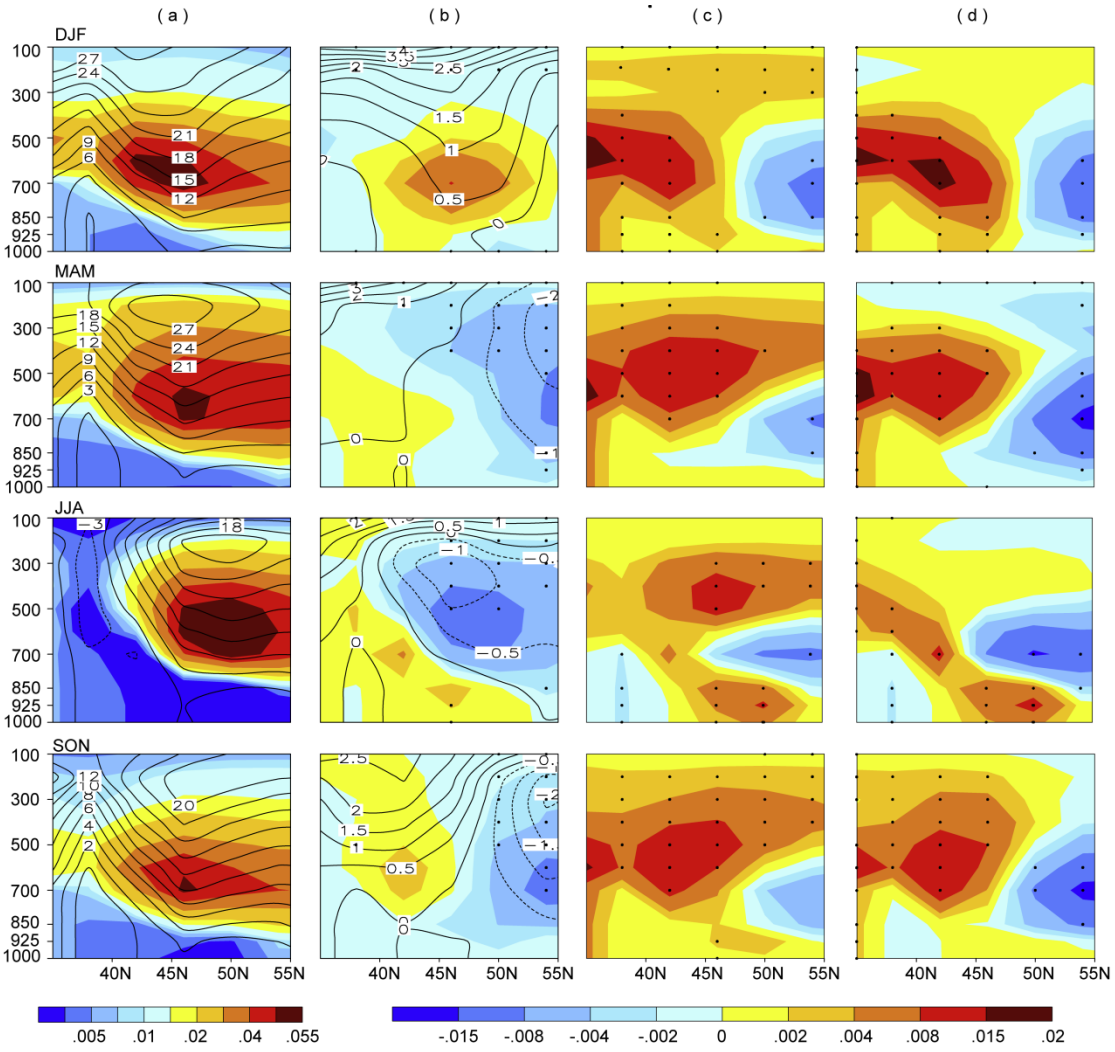

Fig. 12. Same as Figure 11 but mass fluxes and winds are those through the meridional plane along 75°E from 35° to 55°N.

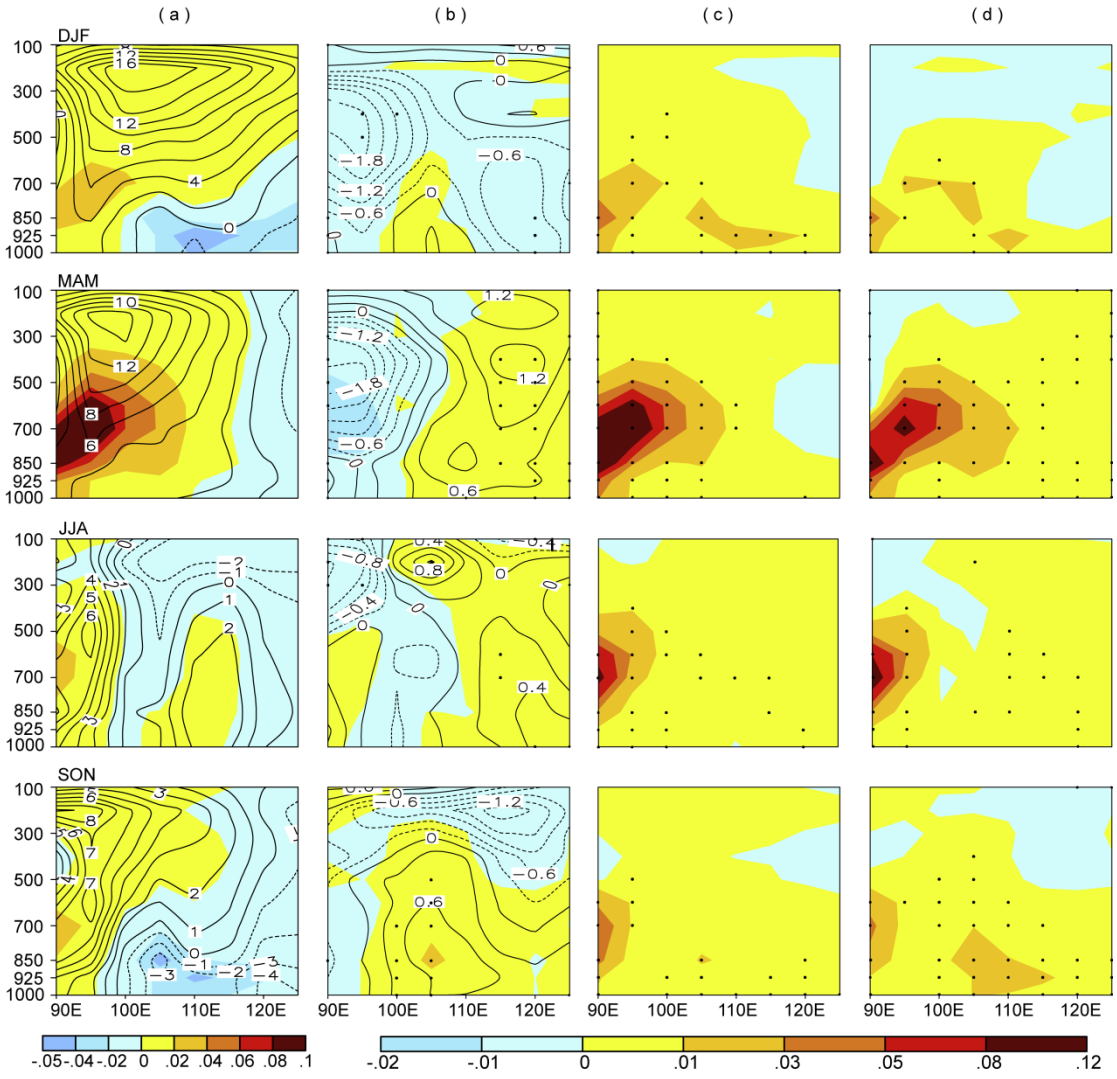

Fig. 13. (a) Simulated present-day mass fluxes of $PM_{2.5}$ and meridional winds. Projected changes in mass fluxes of $PM_{2.5}$ and meridional winds from the present day (1996-2005) to future (2046-2055) owing to (b) climate change alone, (c) changes in anthropogenic emissions alone, and (d) changes in both climate and anthropogenic emissions. Mass fluxes of $PM_{2.5}$ are shown by shades (Units: Tg) and winds are represented by contours (Units: m s^{-1}). Both mass fluxes and winds are those through latitudinal plane along 21.7°N from 90° to 125°E. Positive (negative) fluxes indicate northward (southward) transport. The dotted areas are statistically significant at the 95% level, as determined by the student's two sample t-test.

Supplementary Material

1. Observed concentrations of aerosols in China

Table S1. Observed concentrations of sulfate aerosol in China

Location	Period		Concentration ($\mu g\ m^{-3}$)	Reference	Notes on measurements
Beijing (116.4°E, 39.9°N)	Aug 2001 - Sep 2002	Summer	13.43	Duan et al. (2006)	(1) The $PM_{2.5}$ samples were collected on the roof of a 3-m tall building (about 4.5 m above the ground). The samples were collected integrated weekly.
		Autumn	9.61		
		Winter	9.88		
		Spring	6.71		
Nanjing (118.8°E, 32.0°N)	Sep 2001		11.5	Yang et al. (2005)	(2) The $PM_{2.5}$ samples were collected on the rooftop of a two-story building (8-10 m above the ground). Sampling started at about 8 am and ended at about 8 pm every day; each sample was collected for 12 h.
	Apr 2001		8.79	Wang et al. (2002)	(3) The $PM_{2.5}$ samples were collected 1.5 m above the ground. Sampling started and ended at about 8:30 am and 4:30 pm every day; each sample was collected for 8 h.
	Feb 2001		10.04		
Shanghai (121.5°E, 31.2°N)	Dec 2006 – Jan 2007	Winter	9.52	Fu et al. (2008)	(4) The $PM_{2.5}$ samples were collected on the roof of a building (20 m above the ground). The sampling was from 9:00 am to 9:00 am of the next day for 24 h.
	Jul – Aug 2004	Summer	5.43	Wang et al. (2006)	(5) The $PM_{2.5}$ samples were collected on the roofof a building (~15 m above the ground). The samples were collected in daytime (8:00-20:00) for 12 h.
	Mar – Apr 2004	Spring	11.73		
	Sep – Oct 2003	Antumn	8.7		
Fuzhou (119.3°E, 26.1°N)	Apr 2007 – Jan 2008	Spring	10.14±2.66	Xu et al. (2012)	(6) The samplers were mounted on the rooftop of one office building (about 23 m above the ground). The $PM_{2.5}$ samples were collected for 23 h.
		Summer	6.62±1.51		
		Autumn	11.59±4.28		
		Winter	14.78±6.44		
Hong Kong (114.2°E, 22.3°N)	Nov 2000 – Feb 2001		8.10	Ho et al. (2006)	(7) The $PM_{2.5}$ samples were collected at about 6-8 m above the ground. The samples were collected once every 6 days (each sampling lasted for 24-h).
Qingdao (121°E, 36.5°N)	25 Feb – 15 Mar 2002		11.9	Takami et al. (2006)	(8) The sampling site was about 450 m above the sea level. The sampling of $PM_{2.5}$ was carried out for about 24 h from 8:00 am to the next morning.
	17 Feb – 02 Mar 2001		19.1		
Dalian (121.5°E, 39°N)	2006 to 2007	Spring	11.68	Zhang et al. (2012)	(9) The rural stations were right above the ground level. At the urban
		Summer	15.15		

		Autumn	13.58		locations, the samples were usually collected 50-100 m above the ground. The 24-h aerosol filter samples of PM_{10} (0900 to 0900 local time) were collected every three days at the 16 stations. The observed concentrations listed here were those in Zhang et al. (2012) multiplied by 0.6 to convert PM_{10} to $PM_{2.5}$ following the suggestions in Zhang et al. (2002)
Gaolanshan (105.9°E,36.0°N)	2006 to 2007	Summer	7.08		
		Autumn	11.91		
Jinsha (114.2°E, 29.6°N)	2006 to 2007	Spring	13.35		
Lhasa (91.1°E, 29.7°N)	2006 to 2007	Spring	1.74		
		Summer	1.85		
		Autumn	1.63		
		Winter	2.21		
Lin'an (121.2°E, 31.1°N)	2006 to 2007	Spring	13.16		
		Summer	12.09		
		Autumn	12.95		
		Winter	14.32		
Longfengshan (127.6°E, 44.7°N)	2006 to 2007	Spring	4.69		
		Summer	7.32		
		Autumn	4.73		
		Winter	8.15		
Nanning (108.3°E, 22.8°N)	2006 to 2007	Spring	9.22		
		Winter	14.84		
Panyu (113.4°E, 23.0°N)	2006 to 2007	Winter	16.28		
Taiyangshan (111.7°E, 29.2°N)	2006 to 2007	Spring	11.92		
		Winter	16.59		

Table S2. Observed concentrations of nitrate aerosol in China

Location	Period		Concentration ($\mu g\ m^{-3}$)	Reference	Notes on measurements
Beijing (116.4°E, 39.9°N)	Jul 1999 - Sep 2000	Summer	4.59	He et al. (2001)	(10) The $PM_{2.5}$ samplers were placed on the roof of a 3 m tall building. The samples were collected integrated weekly.
		Spring	7.26		
	2001-2003	Autumn	9.14	Wang et al. (2005)	--
		Winter	12.29		
Nanjing (118.8°E, 32.0°N)	Sep 2001		3.24	Yang et al. (2005)	Same as (2) in Table S1.
	Apr 2001		4.53	Wang et al. (2002)	Same as (3) in Table S1.
	Feb 2001		5.67		
Shanghai (121.5°E, 31.2°N)	20 Mar 1999 -27 Mar 2000	Spring	5.4	Ye et al. (2002)	(11) The site was 16-m above the ground. The samples of $PM_{2.5}$ were collected integrated weekly.
	Jul-Aug 2004	Summer	2.59	Wang et al. (2006)	Same as (5) in Table S1.
	Sep-Oct 2003	Antumn	3.70		
	Dec 2006 - Jan 2007	Winter	6.76	Fu et al. (2008)	Same as (4) in Table S1.
Hangzhou (120.1°E, 30.2°N)	Sep 2001-Aug 2002	Summer	4.68	Cao et al. (2009a)	(12) PM_{10} samples were collected every three days from 8:00 am for 24h.
		Spring	7.20		
		Autumn	7.07		
		Winter	11.19		

Tianjin (117.12°E, 39.4°N)	Jan 2008		16.6	Gu et al. (2011)	(13) The sampling devices were situated about 10 m above the ground. The 24-h (0900 to 0900 local time) samples of $PM_{2.5}$ were collected.
Hong Kong (114.2°E, 22.3°N)	Nov 2000 - Feb 2001		1.20	Ho et al. (2006)	Same as (7) in Table S1.
Fuzhou (119.3°E, 26.1°N)	Apr 2007 – Jan 2008	Autumn	3.13±2.13	Xu et al. (2012)	Same as (6) in Table S1.
		Winter	8.77±3.17		
		Spring	4.60±1.09		
		Summer	1.10±0.35		
Qingdao (121°E, 36.5°N)	25 Feb–15 Mar 2002		10.3	Takami et al. (2006)	Same as (8) in Table S1.
	17 Feb–02 Mar 2001		12.5		
Fenghuanshan (124°E, 40.5°N)	17 Feb–01 Mar, 2001		7.3		
Dalian (121.5°E, 39°N)	2006 to 2007	Spring	8.32	Zhang et al. (2012)	Same as (9) in Table S1.
Dunhuang (94.7°E, 40.2°N)	2006 to 2007	Spring	1.17		
		Autumn	1.37		
		Winter	1.82		
Gucheng (115.8°E, 39.1°N)	2006 to 2007	Spring	10.21		
		Summer	9.75		
		Autumn	12.06		
		Winter	16.30		
Jinsha (114.2°E, 29.6°N)	2006 to 2007	Spring	3.00		
		Autumn	7.10		
		Winter	5.79		
Lhasa (91.1°E, 29.7°N)	2006 to 2007	Spring	1.38		
		Summer	1.25		
		Autumn	1.33		
		Winter	1.39		
Lin'an (121.2°E, 31.1°N)	2006 to 2007	Spring	5.59		
		Summer	3.37		
		Autumn	5.06		
		Winter	6.99		
Longfengshan (127.6°E, 44.7°N)	2006 to 2007	Spring	2.43		
		Summer	1.44		
		Autumn	2.50		
		Winter	5.42		
Nanning (108.3°E, 22.8°N)	2006 to 2007	Spring	2.92		
		Autumn	3.00		
		Winter	4.39		
Panyu (113.4°E, 23.0°N)	2006 to 2007	Winter	8.83		
Taiyangshan (111.7°E, 19.2°N)	2006 to 2007	Spring	3.01		
		Autumn	7.57		
		Winter	5.73		
Xi'an (108.6°E, 34.3°N)	2006 to 2007	Winter	14.79		

Table S3. Observed concentrations of BC aerosol in China

Location	Period		Concentration ($\mu g\ m^{-3}$)	Reference	Notes on measurements
Beijing (116.4°E, 39.9°N)	Jul 1999 - Sep 2000	Spring	6.67	He et al. (2001)	Same as (10) in Table S2.
	Jan-Jul 2003	Summer	4.6±3.0	Cao et al. (2007)	(14) The samplers were set up on rooftops at varying heights 6-20 m above the ground. The sampling time period of $PM_{2.5}$ was 24 h (9 am to 9 am local time).
		Winter	7.1±3.5		
Nanjing (118.8°E , 32.0°N)	Feb 2001 – Sep 2001	Feb	2.88	Yang et al. (2005)	Same as (2) in Table S1.
		Sep	4.01		
Shanghai (121.5°E, 31.2°N)	Apr 2006 –Jan 2007	Summer	1.1	Hou et al. (2011)	(15) The $PM_{2.5}$ samples were collected on the roof of NO.4 teaching building at Fudan University. The sampling time period was generally 24 h.
		Autumn	2.1		
	Oct 2005-Jul 2006	Spring	3.1±1.5	Feng et al. (2009)	(16) The sampler was mounted about 10 m abve the ground. During the four weeks of each sampling month, 24-h $PM_{2.5}$ samples (from morning to morning) were collected.
		Winter	2.3±1.0		
Hangzhou (120.1°E, 30.2°N)	Sep 2001 – Aug 2002	Winter	4.43	Cao et al. (2009a)	Same as (12) in Table S2.
		Summer	2.82		
		Spring	2.96		
		Autumn	4.38		
Changchun (125.3°E, 43.9°N)	Jan - Jul 2003	Summer	2.9±1.4	Cao et al. (2007)	Same as (14) in Table S3.
Qingdao (120.3°E, 36.0°N)	Jan - Jul 2003	Winter	6.3±2.4		
		Summer	1.4±0.5		
HongKong (114.1°E, 22.2°N)	Jan - Jul 2003	Winter	5.8±2.6		
Wuhan (114.2°E, 30.5°N)	Jan - Jul 2003	Summer	3.0±0.07		
Xiamen (118.1°E, 24.4°N)	Jan - Jul 2003	Winter	5.0±1.4		
		Summer	1.4±1.3		
Sheshan (131.2°E, 31.1°N)	Oct – Nov 1999		3.2±1.9	Xu et al. (2002)	(17) The sampler was located on the roof of the monitoring room, and at a height ~7 m above the ground. Daily $PM_{2.5}$ filter samples were collected at 9:00 am to the next morning for 24h.
Changshu (120.8°E, 31.7°N)	Oct – Nov 1999		3.6±1.7		
Akdala (87.97°E, 47.1°N)	Jan-Mar 2005		0.33	Qu et al. (2008)	(18) PM_{10} aerosol samples were collected from a 5 m tall building (3583 above the sea level). The sampling period was 72 hr (normally from 8:00-8:00).
Muztagh (75.01°E, 38.3°N)	2005		0.051	Cao et al. (2009b)	(19) Each filter sample of TSP was nominally collected over a one week period at 4500 m above the sea level.
Zhuzhang (99.72°E, 28°N)	Jan-Feb 2005		0.35	Qu et al. (2008)	Same as (18) in Table S3.

Dalian (121.5°E, 39°N)	2006 to 2007	Spring	2.74	Zhang et al. (2012)	Same as (9) in Table S1.
		Summer	2.12		
		Autumn	3.27		
		Winter	4.53		
Gaolanshan (105.9°E,36.0°N)	2006 to 2007	Summer	1.73		
		Autumn	2.44		
Gucheng (115.8°E, 39.1°N)	2006 to 2007	Spring	4.18		
		Summer	4.24		
		Autumn	6.96		
Jinsha (114.2°E, 29.6°N)	2006 to 2007	Spring	1.35		
		Summer	1.14		
		Autumn	2.58		
		Winter	2.07		
Lhasa (91.1°E, 29.7°N)	2006 to 2007	Spring	1.82		
		Summer	2.09		
		Autumn	2.10		
		Winter	3.27		
Lin'an (121.2°E, 31.1°N)	2006 to 2007	Spring	2.51		
		Summer	2.25		
		Autumn	2.49		
		Winter	2.91		
Longfengshan (127.6°E, 44.7°N)	2006 to 2007	Spring	0.92		
		Summer	0.67		
		Autumn	1.51		
		Winter	2.30		
Nanning (108.3°E, 22.8°N)	2006 to 2007	Spring	1.58		
		Summer	1.64		
		Autumn	3.00		
		Winter	2.99		
Panyu (113.4°E, 23.0°N)	2006 to 2007	Spring	4.90		
		Summer	2.92		
		Autumn	4.48		
		Winter	5.80		
Taiyangshan (111.7°E, 19.2°N)	2006 to 2007	Spring	1.23		
		Summer	1.26		
		Autumn	2.20		
		Winter	1.57		
Xi'an (108.9°E, 34.3°N)	2006 to 2007	Summer	4.56		
		Autumn	6.49		
Zhengzhou (113.7°E, 34.8°N)	2006 to 2007	Spring	4.84		
		Summer	4.18		
		Autumn	5.96		

Table S4. Observed concentrations of OC aerosol in China

Location	Period		Concentration ($\mu g\ m^{-3}$)	Reference	Notes on measurements
Beijing (116.4°E, 39.9°N)	Jul 1999 - Sep2000	Summer	13.42	He et al. (2001)	Same as (10) in Table S2.
		Spring	18.21		
Nanjing	2001	Feb	18.34	Wang et al.	Same as (3) in Table S1.

(118.8°E, 32.0°N)		Apr	20.14	(2002)	
Shanghai (121.5°E, 31.2°N)	Apr 2006 –Jan 2007	Spring	8.4±2.2	Hou et al. (2011)	Same as (15) in Table S3.
		Summer	3.8±1.6		
		Autumn	6.5±2.6		
		Winter	10.9±4.5		
Hangzhou (120.1°E, 30.2°N)	Sep 2001 – Aug 2002	Winter	23.81	Cao et al. (2009a)	Same as (12) in Table S2.
		summer	13.54		
		spring	14.03		
Changchun (125.3°E, 43.9°N)	Jan - Jul 2003	Summer	12.5±5.2	Cao et al. (2007)	Same as (14) in Table S3.
Qingdao (120.3°E, 36.0°N)	Jan - Jul 2003	Summer	5.0±2.9		
Tianjin (117.2°E, 39.1°N)	Jan - Jul 2003	Summer	16.5±4.1		
HongKong (114.1°E, 22.2°N)	Jan - Jul 2003	Winter	11.2±4.8		
		Summer	7.3±1.9		
Wuhan (114.2°E, 30.5°N)	Jan - Jul 2003	Summer	14.2±3.7		
Xiamen (118.1°E, 24.4°N)	Jan - Jul 2003	Winter	16.5±5.4		
Muztagh (75.01°E, 38.3°N)	2005		0.51	Cao et al. (2009b)	Same as (19) in Table S3.
Zhuzhang (99.72°E, 28°N)	Jan-Feb 2005		3.1	Qu et al. (2008)	Same as (18) in Table S3.
Chengdu (104.1°E, 30.6°N)	2006 to 2007	Spring	22.82	Zhang et al. (2012)	Same as (9) in Table S1.
Dalian (121.5°E, 39°N)	2006 to 2007	Spring	14.10		
		Summer	9.03		
		Autumn	10.71		
		Winter	13.90		
Gaolanshan (105.9°E,36.0°N)	2006 to 2007	Summer	9.44		
Gucheng (115.8°E, 39.1°N)	2006 to 2007	Spring	15.43		
		Summer	12.90		
Jinsha (114.2°E, 29.6°N)	2006 to 2007	Spring	8.09		
		Summer	7.20		
		Winter	10.17		
Lhasa (91.1°E, 29.7°N)	2006 to 2007	Spring	12.11		
		Autumn	11.48		
		Winter	17.89		
Lin'an (121.2°E, 31.1°N)	2006 to 2007	Spring	9.15		
		Summer	8.08		
		Autumn	8.77		
		Winter	10.57		
Longfengshan (127.6°E, 44.7°N)	2006 to	Spring	7.71		
		Summer	5.79		

	2007	Autumn	11.22		
		Winter	13.01		
Nanning (108.3°E, 22.8°N)	2006 to 2007	Spring	7.75		
		Summer	8.03		
		Autumn	12.67		
		Winter	13.22		
Panyu (113.4°E, 23.0°N)	2006 to 2007	Spring	12.33		
		Winter	16.36		
Taiyangshan (111.7°E, 19.2°N)	2006 to 2007	Spring	6.89		
		Summer	6.84		
		Autumn	10.17		
		Winter	7.95		
Xi'an (108.9°E, 34.3°N)	2006 to 2007	Summer	16.86		
Zhengzhou (113.7°E, 34.8°N)	2006 to 2007	Summer	12.03		
		Autumn	19.65		

Note: A spreadsheet file of aerosol measurements can be obtained by contacting the corresponding author of the paper (hongliao@mail.iap.ac.cn).

References

Cao, J. J., Lee, S. C., Chow, J. C., Watson, J. G., Ho, K. F., Zhang, R. J., Jin, Z. D., Shen, Z. X., Chen, G. C., Kang, Y. M., Zou, S. C., Zhang, L. Z., Qi, S. H., Dai, M. H., Cheng, Y., and Hu, K.: Spatial and seasonal distributions of carbonaceous aerosols over China, J Geophys Res-Atmos, 112, Artn D22s11, Doi 10.1029/2006jd008205, 2007.

Cao, J. J., Shen, Z. X., Chow, J. C., Qi, G. W., and Watson, J. G.: Seasonal variations and sources of mass and chemical composition for PM10 aerosol in Hangzhou, China, Particuology, 7, 161-168, DOI 10.1016/j.partic.2009.01.009, 2009a.

Cao, J. J., Xu, B. Q., He, J. Q., Liu, X. Q., Han, Y. M., Wang, G. H., and Zhu, C. S.: Concentrations, seasonal variations, and transport of carbonaceous aerosol at a remote Mountainous region in western China, Atmos. Environ., 43, 4444–4452, doi:10.1016/j.atmosenv.2009.06.023, 2009b.

Duan, F. K., He, K. B., Ma, Y. L., Yang, F. M., Yu, X. C., Cadle, S. H., Chan, T., and Mulawa, P. A.: Concentration and chemical characteristics of PM2.5 in Beijing, China: 2001-2002, Sci Total Environ, 355, 264-275, DOI 10.1016/j.scitotenv.2005.03.001, 2006.

Feng, Y. L., Chen, Y. J., Guo, H., Zhi, G. R., Xiong, S. C., Li, J., Sheng, G. Y., and Fu, J. M.: Characteristics of organic and elemental carbon in PM2.5 samples in Shanghai, China, Atmos Res, 92, 434-442, DOI 10.1016/j.atmosres.2009.01.003, 2009.

Fu, Q. Y., Zhuang, G. S., Wang, J., Xu, C., Huang, K., Li, J., Hou, B., Lu, T., and Streets, D. G.: Mechanism of formation of the heaviest pollution episode ever recorded in the Yangtze River Delta, China, Atmospheric Environment, 42, 2023-2036, DOI 10.1016/j.atmosenv.2007.12.002, 2008.

Gu, J. X., Bai, Z. P., Li, W. F., Wu, L. P., Liu, A. X., Dong, H. Y., and Xie, Y. Y.: Chemical composition of PM2.5 during winter in Tianjin, China, Particuology, 9, 215-221, DOI 10.1016/j.partic.2011.03.001, 2011.

He, K. B., Yang, F. M., Ma, Y. L., Zhang, Q., Yao, X. H., Chan, C. K., Cadle, S., Chan, T., and Mulawa, P.: The characteristics of PM2.5 in Beijing, China, Atmospheric Environment, 35, 4959-4970, Doi 10.1016/S1352-2310(01)00301-6, 2001.

Ho, K. F., Cao, J. J., Lee, S. C., and Chan, C. K.: Source apportionment of PM2.5 in urban area of Hong Kong, J Hazard Mater, 138, 73-85, DOI 10.1016/j.jhazmat.2006.05.047, 2006.

Hou, B., Zhuang, G., Zhang, R., Liu, T., Guo, Z., and Chen, Y.: The implication of carbonaceous aerosol to the formation of haze: revealed from the characteristics and sources of OC/EC over a mega-city in China, J Hazard Mater, 190, 529-536, 10.1016/j.jhazmat.2011.03.072, 2011.

Qu, W. J., Zhang, X. Y., Arimoto, R., Wang, D., Wang, Y. Q., Yan, L. W., and Li, Y.: Chemical composition of the background aerosol at two sites in southwestern and northwestern China: potential influences of regional transport, Tellus, 60B, 657–673, doi:10.1111/j.1600-0889.2008.00342.x, 2008.

Takami, A., Wang, W., Tang, D. G., and Hatakeyama, S.: Measurements of gas and aerosol for two weeks in northern China during the winter-spring period of 2000, 2001 and 2002, Atmos Res, 82, 688-697, DOI 10.1016/j.atmosres.2006.02.023, 2006.

Wang, G. H., Huang, L. M., Gao, S. X., Gao, S. T., and Wang, L. S.: Characterization of water-soluble species of PM10 and PM2.5 aerosols in urban area in Nanjing, China, Atmospheric Environment, 36, 1299-1307, Pii S1352-2310(01)00550-7, Doi 10.1016/S1352-2310(01)00550-7, 2002.

Wang, W.G., J. Wu, andN. Liu, 2005: Researches on the influence of pollution emission on tropospheric ozone variation and radiation over China and its adjacent area, Chinese .J. Atmos. Sci. (in Chinese), 29(5), 734–746.

Wang, Y., Zhuang, G. S., Zhang, X. Y., Huang, K., Xu, C., Tang, A. H., Chen, J. M., and An, Z. S.: The ion chemistry, seasonal cycle, and sources of PM2.5 and TSP aerosol in Shanghai, Atmospheric Environment, 40, 2935-2952, DOI 10.1016/j.atmosenv.2005.12.051, 2006.

Xu, J., Bergin, M. H., Yu, X., Liu, G., Zhao, J., Carrico, C. M., and Baumann, K.: Measurement of aerosol chemical, physical and radiative properties in the Yangtze delta region of China, Atmospheric Environment, 36, 161-173, Doi 10.1016/S1352-2310(01)00455-1, 2002.

Xu, L. L., Chen, X. Q., Chen, J. S., Zhang, F. W., He, C., Zhao, J. P., and Yin, L. Q.: Seasonal variations and chemical compositions of PM2.5 aerosol in the urban area of Fuzhou, China, Atmos Res, 104, 264-272, DOI 10.1016/j.atmosres.2011.10.017, 2012.

Yang, H., Yu, J. Z., Ho, S. S. H., Xu, J., Wu, W.-S., Wan, C. H., Wang, X., Wang, X., and Wang, L.: The chemical composition of inorganic and carbonaceous materials in PM2.5 in Nanjing, China, Atmospheric Environment, 39, 3735-3749, 10.1016/j.atmosenv.2005.03.010, 2005.

Ye, B. M., Ji, X. L., Yang, H. Z., Yao, X. H., Chan, C. K., Cadle, S. H., Chan, T., and Mulawa, P. A.: Concentration and chemical composition of PM2.5 in Shanghai for a 1-year period,

Atmospheric Environment, 37, 499-510, Pii S1352-2310(02)00918-4, Doi 10.1016/S1352-2310(02)00918-4, 2003.

Zhang, X. Y., Cao, J. J., Li, L. M., Arimoto, R., Cheng, Y., Huebert, B., and Wang, D.: Characterization of Atmospheric Aerosol over XiAn in the South Margin of the Loess Plateau, China, Atmospheric Environment, 36, 4189-4199, Pii S1352-2310(02)00347-3, Doi 10.1016/S1352-2310(02)00347-3, 2002.

Zhang, X.Y., Wang, Y.Q., Niu, T., Zhang, X. C., Gong, S. L., Zhang, Y. M., and Sun, J. Y.: Atmospheric aerosol compositions in China: Spatial/temporal variability, chemical signature, regional haze distribution and comparisons with global aerosols, Atmos. Chem. Phys, 12,779-799, doi:10.5194/acp-12-779-2012, 2012.

2. Comparisons of simulated (GISS Model 3) and reanalyzed (GEOS-4) surface air temperature, zonal wind, and precipitation for present-day (1996-2005)

Both the simulated and assimilated surface air temperatures show higher temperatures in southern China than in northern China and also higher temperatures in eastern China than in western China (Figure A). The maximum temperatures in southeastern China are simulated to be 280–290 K in DJF, 290–300 K in MAM, 300–310 K in JJA, and 290–300 K in SON, which agree with the assimilated values in all seasons except that the assimilated maximum temperatures in southeastern China are lower than 305 K in JJA. Simulated zonal winds averaged over 100°–120°E longitudes show maximum wind speeds of the jet stream located at 200 hPa altitude of 60, 40, 20, and 30 m s^{-1} in DJF, MAM, JJA, and SON, respectively, which agree closely with the assimilated values (Figure B). The present-day precipitation simulated by the GISS model shows larger values in MAM and JJA than in DJF and SON, which agree with the assimilated precipitation, but the model overestimates precipitation in the middle and lower reaches of the Yangtze River in MAM whereas underestimates precipitation in that region in JJA (Figure C).

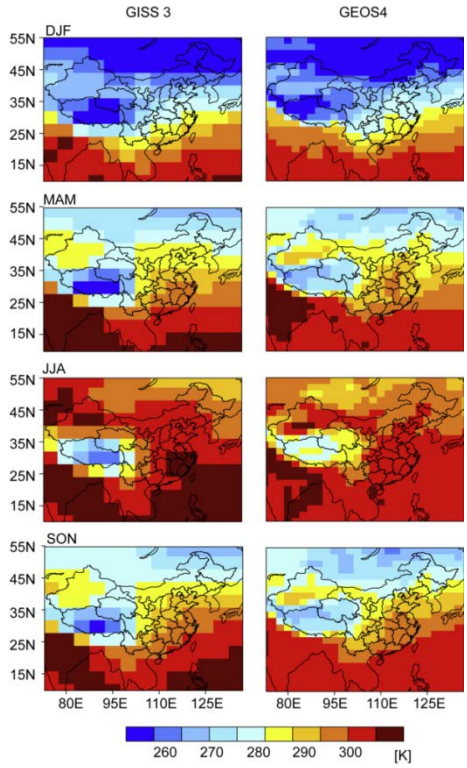

Figure A. Comparisons of simulated (GISS Model 3) and reanalyzed (GEOS-4) surface air temperatures (K) in China for present day (averages over 1996-2005).

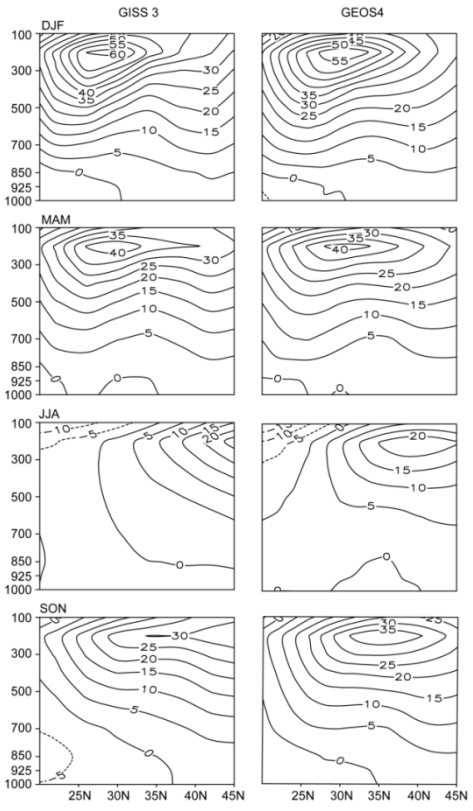

Figure B. Comparisons of simulated (GISS Model 3) and reanalyzed (GEOS-4) zonal winds (m s^{-1}) for present day (averages over 1996-2005). To represent winds over eastern China, winds are averaged over the longitude range of 100°-120°E.

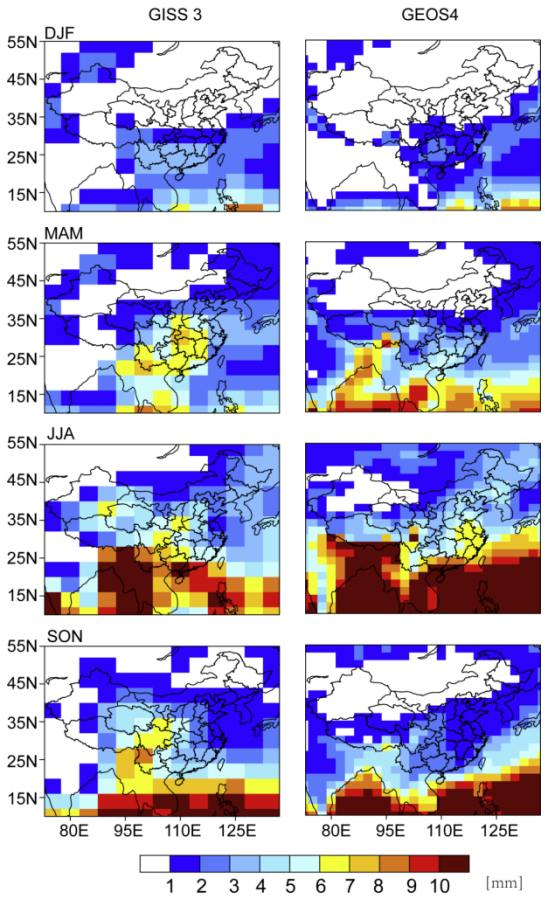

Figure C. Comparisons of simulated (GISS Model 3) and reanalyzed (GEOS-4) precipitation (mm) in China for present day (averages over 1996-2005).

3. The altitude-latitude cross-sections of the changes in aerosol concentrations from the present day to future owing to changes in anthropogenic emissions alone

For the case with changes in emissions alone, since changes in emissions are mostly imposed near the surface, the vertical changes in concentrations of aerosols in the lower troposphere generally follow the sign of changes at the surface-layer, as shown by the altitude-latitude cross-sections of the changes in aerosol concentrations averaged over eastern China (Figure D). Changes in concentrations above 2 km altitude can be influenced by long-range transport. Because our manuscript is already very long, we do not show such plots of vertical changes in concentrations in the manuscript. Instead, we show future changes in long-range transport owing to changes in emissions alone in Figs. 11-13 of the manuscript.

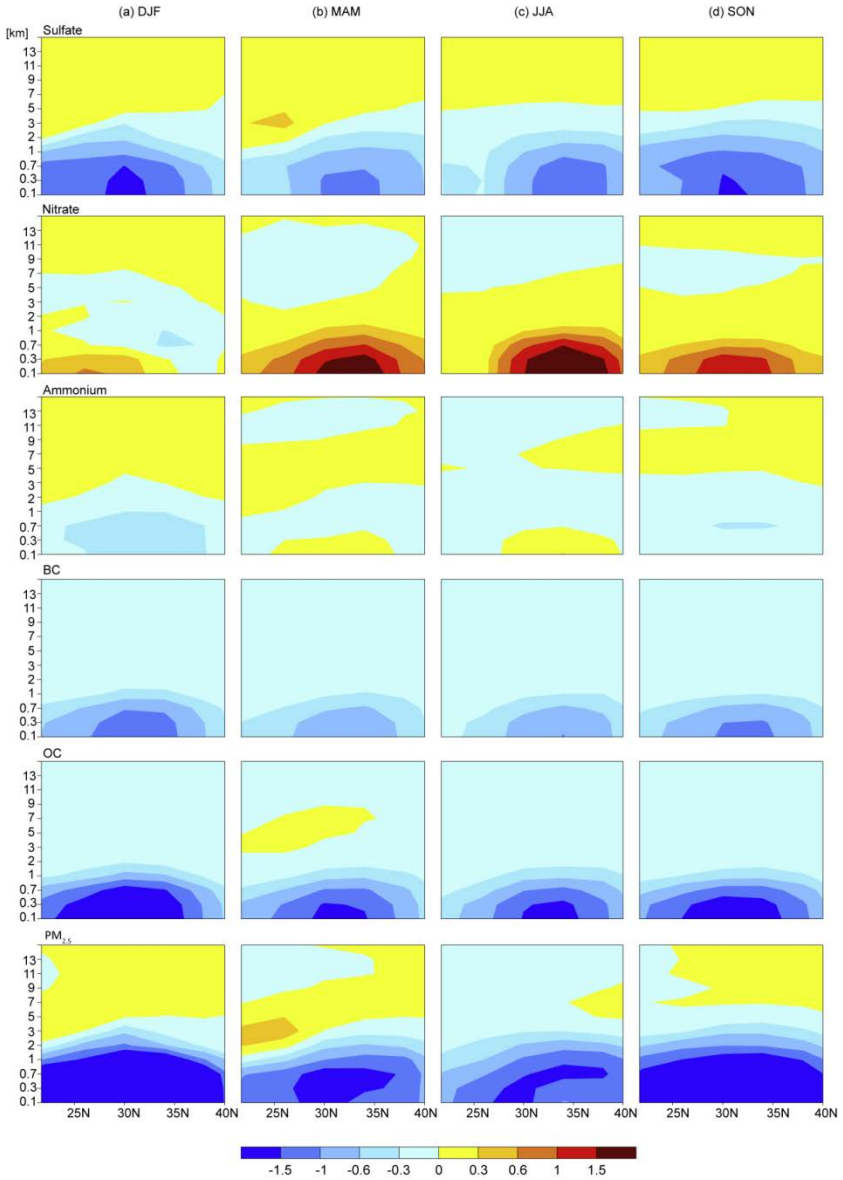

Figure D. The altitude-latitude cross-sections of the changes in aerosol concentrations from the present day (1996-2005) to future (2046-2055) owing to changes in anthropogenic emissions alone. Values are averaged over longitudes from 115°E to 120°E.

4. Explanation about the future changes in PBL depth

The changes in PBL depth result from the simulated changes in atmospheric temperature (or atmospheric stability). As an example, we show in Figure E the 2000-2050 changes in SON air temperatures averaged over 110-120°E and 32-40°N (this area shows large reductions in PBL depth in Figure 4 of the manuscript in SON). The simulated increases in temperature in the 500-700 hPa altitude are larger than those in the lower troposphere, leading to a more stable atmosphere and hence a lower PBL depth in 2050. It should be noted that the negative changes in PBL depth were also found for the US in Pye et al. (2009), with the changes in PBL also simulated by the GISS Model 3.

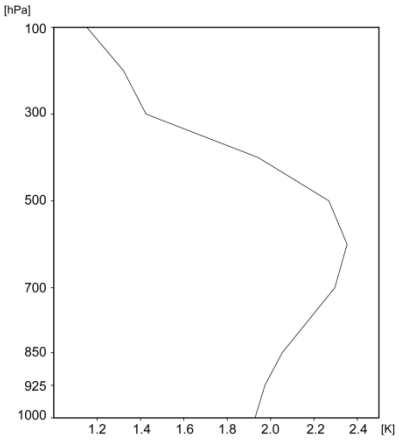

Figure E. The simulated 2000-2050 changes in SON air temperatures averaged over 110-120°E and 32-40°N.

References

Pye, H. O. T., Liao, H.,Wu, S., Mickley, L. J., Jacob, D. J., Henze, D. K., and Seinfeld, J. H.: Effect of changes in climate and emissions on future sulfate-nitrate-ammonium aerosol levels in the United States, J. Geophys. Res.-Atmos., 114, D01205, doi:10.1029/2008jd010701, 2009.